Numerical modelling of the geologically reconstructed Oer-IJ estuary.

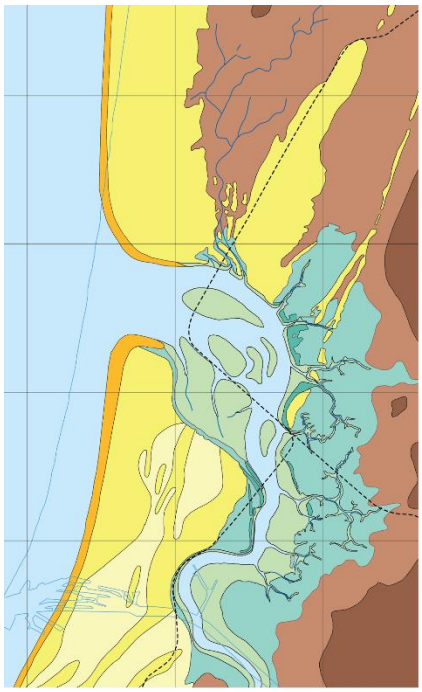

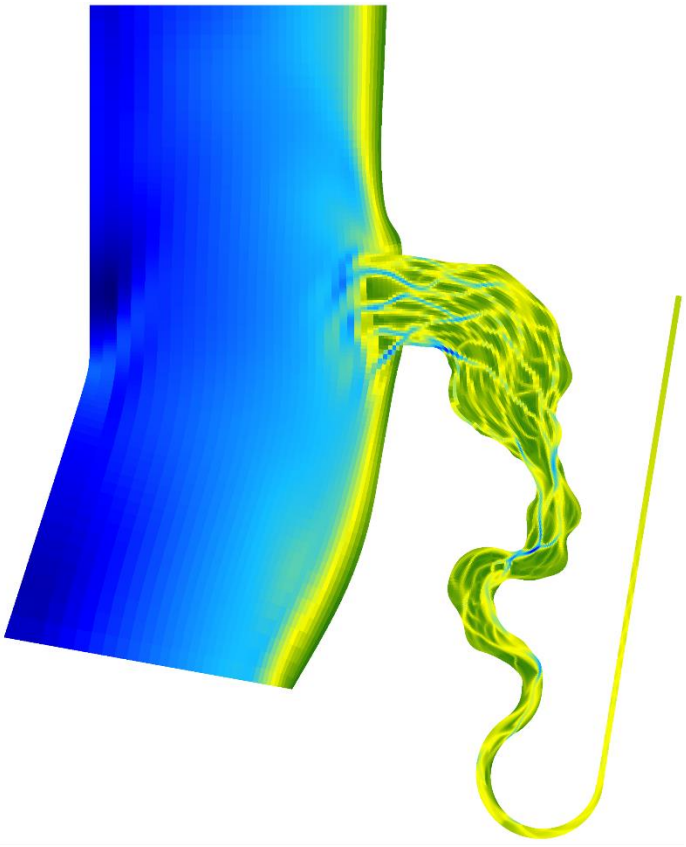

MSc Thesis

Bas Bodewes
Student number: 3507874

June 2013 – December 2014

Master: Earth Surface and Water
Track: Coastal dynamics and fluvial systems

Supervisors: Prof. Dr. M.G. Kleinhans[1], Dr Maarten van der Vegt[1]
[1]*University Utrecht*

Abstract

The Oer-IJ estuary near Castricum was active between 2500 BC and 200 BC. Geologic reconstruction resulted in paleographical maps and in hypotheses explaining its development and closure. The shape of the estuary was convergent, but with an uncharacteristic bend over the entire estuary that was perhaps caused by the washover-type initiation of the estuary. Reconstruction suggests that in the lower estuary bars were present. The estuary was connected with the Hollandse Vecht river and the Almere lake, which must have provided freshwater but barely bed sediment. The reconstruction showed that a period of activity, represented by intertidal bars and a widely extended estuary between 650 and 200 BC coincided with the activity of the Vecht river and the closure of the estuary after 200 BC coincides approximately with the opening of the Vlie inlet, which connects lake Almere with the Waddensea and the North Sea. This leads to the hypothesis that the freshwater inflow kept the estuary open and that tidal bars form in the outer part of the estuary (Vos et al. 2010).

This study will systematically test the hypotheses raised by geologic reconstructions by scenario modelling in Delft3D, in depth averaged approach. The model consist of a 45 km long confined curvilinear grid based on the geologic reconstruction. Tidal components M2, M4 and O1 were applied at the offshore boundary, realistic river discharge up to 500 m^3/s was prescribed at the landward boundary. The influence of the relative curved Oer-IJ estuary shape was tested with similar straightened and similar idealized grids.

Model results show similar results in bar and channel pattern along the estuary for all model settings. Increased river discharge has primary an effect on bed level elevation in the middle of the estuary, which increases with higher discharges. The bended estuary reduces tidal range rapidly in particular when combined with high discharges.

The study concludes that the effect of river discharge on tidal inflow and on estuary filling is significant even when fluvial discharge is only ten percent of the tidal discharge. The bended estuary possibly reflect a part of the tidal energy but definitely reduces tidal influences in the inner part of the estuary. Nevertheless this study shows that river flow is not a prerequisite to keep the estuary open.

Content

List of Figures

List of Tables

Introduction

The Dutch subsurface is the best documented area in the world. The density of geologic information in the direct subsurface is vast, in particular in the river area of the Netherlands. Knowledge on the subsurface of coastal areas is less well documented and limited to specific areas in the Netherlands (Van der Spek 1995; Vos 2012). These studies have extended knowledge about the subsurface at locations of their cores, they lack information between individual cores. These gaps are filled by interpretation and knowledge of present day systems and as such generate geological reconstruction maps. Interpretation is often limited in systems where variation along one axis is relative small or constant, such as floodplains along rivers where variation is primary found along an axis perpendicular to the river. However estuarine systems are complex and dynamic along multiple axis' of the system, estuarine systems vary both perpendicular, longitudinal as well along the vertical. As such interpretation in between cores are less scripted and interpretation can be more variable.

Moreover these cores can only deliver specific information in the margins of the estuarine area, in particular by vegetation about for instance water level. In the center of the estuary they lack knowledge as cores often only record the deepest channel remnants as bars in a dynamic system tend to be eroded when channels migrate. As a result bars are only recorded in cores in the end phase of the system and information is lacking about bars at times of the main activity of the estuary. The subdivision between sub- and intertidal areas as such is the result of interpretation, and only partly founded cores along the margins of the estuary.

Estuarine morphologic modelling is nowadays often used to understand estuarine dynamics (Van der Wegen et al. 2010) as well to predict future behavior of estuarine systems. In modelling studies intermediate time steps can easily be extracted and compared, as such these studies can strongly visualize the dynamic behavior of an estuarine system. In contrast these modelling studies have their limits, models are often very dependent on initial and boundary conditions as well are subject to uncertainties in the underlying physics. Despite this great opportunity, these models have their shortcoming too. Parameters and boundary conditions are often simplified to speed up computation time and initial conditions are important in the progress of a model. Models can be validated when extended time series exist of bathymetry or hydrodynamics, such information nevertheless barely exists in present day estuaries over longer periods.

The objective of this study is to combine this extensive geologic knowledge with estuarine numerical modelling. The set-up of this study is not unique (Kleinhans et al. 2010), although the use of a geologic reconstruction (Vos 2012) of the Oer-IJ estuary in combination with numerical depth-averaged modelling is not done before on this estuary. Recent modelling studies focus mainly on the present day estuaries, either on future or on past decades (Dam et al. 2007). While geologic studies either neglect knowledge on hydro and morphodynamic processes or are unaware of the use of modelling studies for their goals. This study will test interpretations, mainly in the intertidal area, in the geologic reconstruction and investigate as well the effect of specified boundary conditions on modelling results.

This introduction is followed by an overview of the area of research as well a geologic reconstruction of the area. It is followed by an overview of what is known about estuarine morphology and morphologic modelling. This section is finished with an overview of the research questions. The report will follow up with a set-up of the study as well a description of the methods used to gather the results. The results will be showed thereafter. In the discussion the effects and uncertainties in the results will be discussed as well the coupling between the results and the geologic reconstruction. The discussion is followed by a conclusion.

Literature Overview

Area of research

Part of the Holocene the Oer-IJ was an active estuary in the Netherlands, located in Noord-Holland (Figure 1). In the main period of activity the mouth of the estuary was located at present day Castricum. The inner part of the estuary converged towards the south, were it was characterized by relative sharp bended meander like pattern, and eventually turned east near present day Noordzeekanaal. In the main period of activity the estuary was connected to the hinterland by the Vecht (Hollandse) river and to peat lakes that are precedents of the Zuiderzee. At present the estuary is filled up and inactive, remnants can nevertheless still be distinguished in the digital elevation model (Figure 1). Elongated elevation differences are visible in agricultural fields which relate to former tidal channels or creeks. The location of the main estuary is distinguished by a decreased elevation compared to its surroundings. Villages like Castricum, Uitgeest, Heemskerk and Beverwijk were build and extended into the former estuary. In particular more recent build parts have been investigated for geology and archeology prior to construction works. This research combines with earlier research results in a large database of geologic and archeological information which is used to make an extensive geologic reconstruction of the area (Vos 2012). This reconstruction is used as basis for the modelling study and as such the related parts of this study will be given in an extensive overview in the next section.

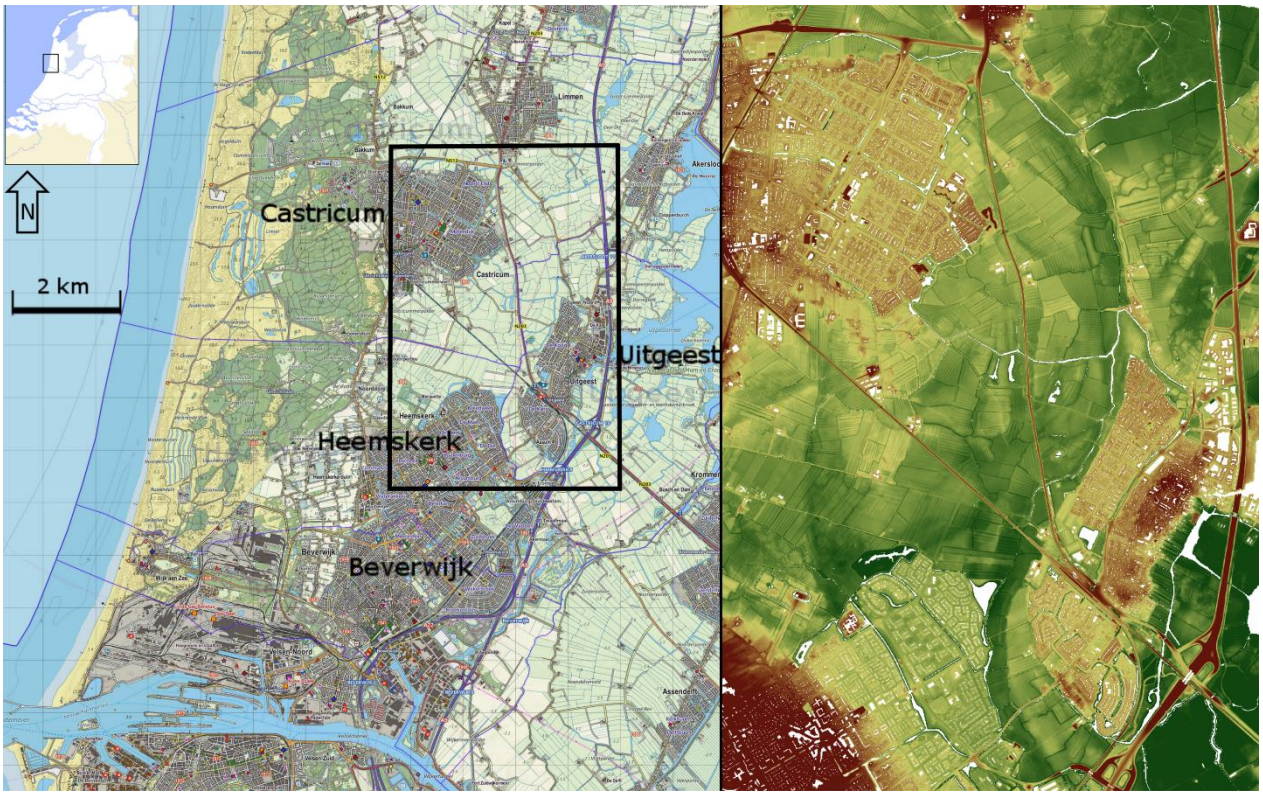

Figure 1: Topographical map (Top33) of the former Oer-IJ area (left) and partial AHN2 map of the Oer-IJ area of interest (right). Red color indicates high elevation, green color indicates low elevation.

Geologic reconstruction Oer-IJ estuary

At the start of the Holocene sea level was relative low, roughly 30 m below the present level and the coastline was situated seaward of the present day coastline. The area behind the coastline was relative dry and incised by several valleys. In Noord-Holland an incised valley was located in east-west direction and included the area of the Oer-IJ. This valley was located at 22-20 m below present level at the Oer-IJ area.

The early Holocene is characterized by fast sea level rise, which caused peat formation in the valley from 7000 BC. In succession the valley drowned due persisting sea level rise and eventually became an inland sea. The sea level rise continued most of the Holocene, nevertheless the rate decreased gradually. The decreasing rate of sea level rise gave rivers like the Overijsselse Vecht a.o., the opportunity to deliver enough sediment and keep up with sea level rise, thereby halting further transgression. At the end of the Atlanticum sea level rise decreased further and the supply of sediment caused peat to grow further west as well regression of the coastline. More seaward, close to the present coastline, beach barriers formed and the inland sea became a tidal inlet with initially two outlets; tidal inlet of Bergen and tidal inlet of Haarlem. The hinterland of both tidal inlets got separated and both estuaries started to silt up. The tidal inlet of Haarlem, a predecessor of the Oer-IJ estuary, silted up roughly 3000 BC.

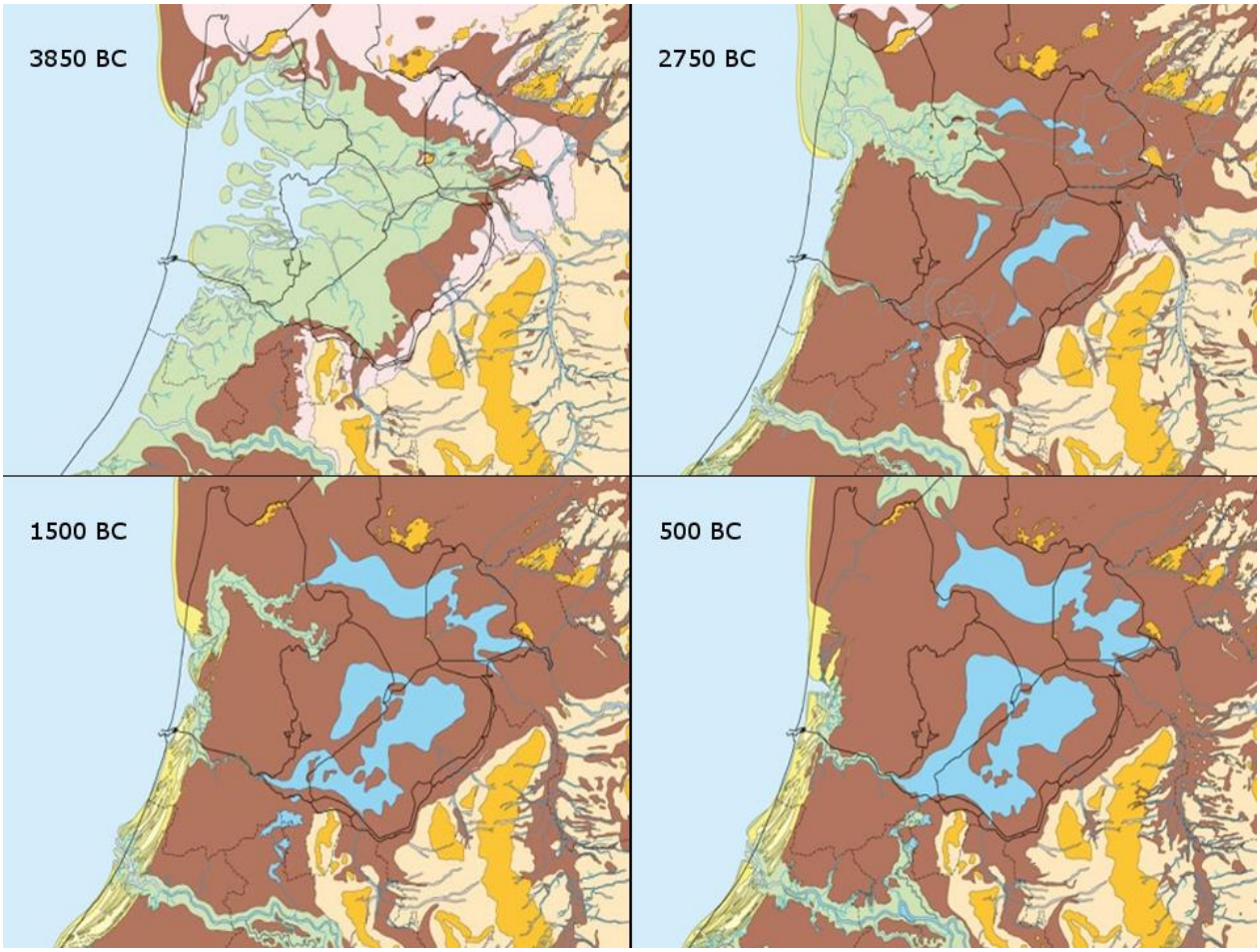

Figure 2: Geologic reconstruction of the surrounding area of the Oer-IJ in four time slices (Vos et al. 2011). Colors indicate geologic units (light blue: salt water; dark blue: fresh water; brown: peat; light green: clay; light yellow: dunes; other colors: Pleistocene deposits). Black lines indicate present day land/water boundaries.

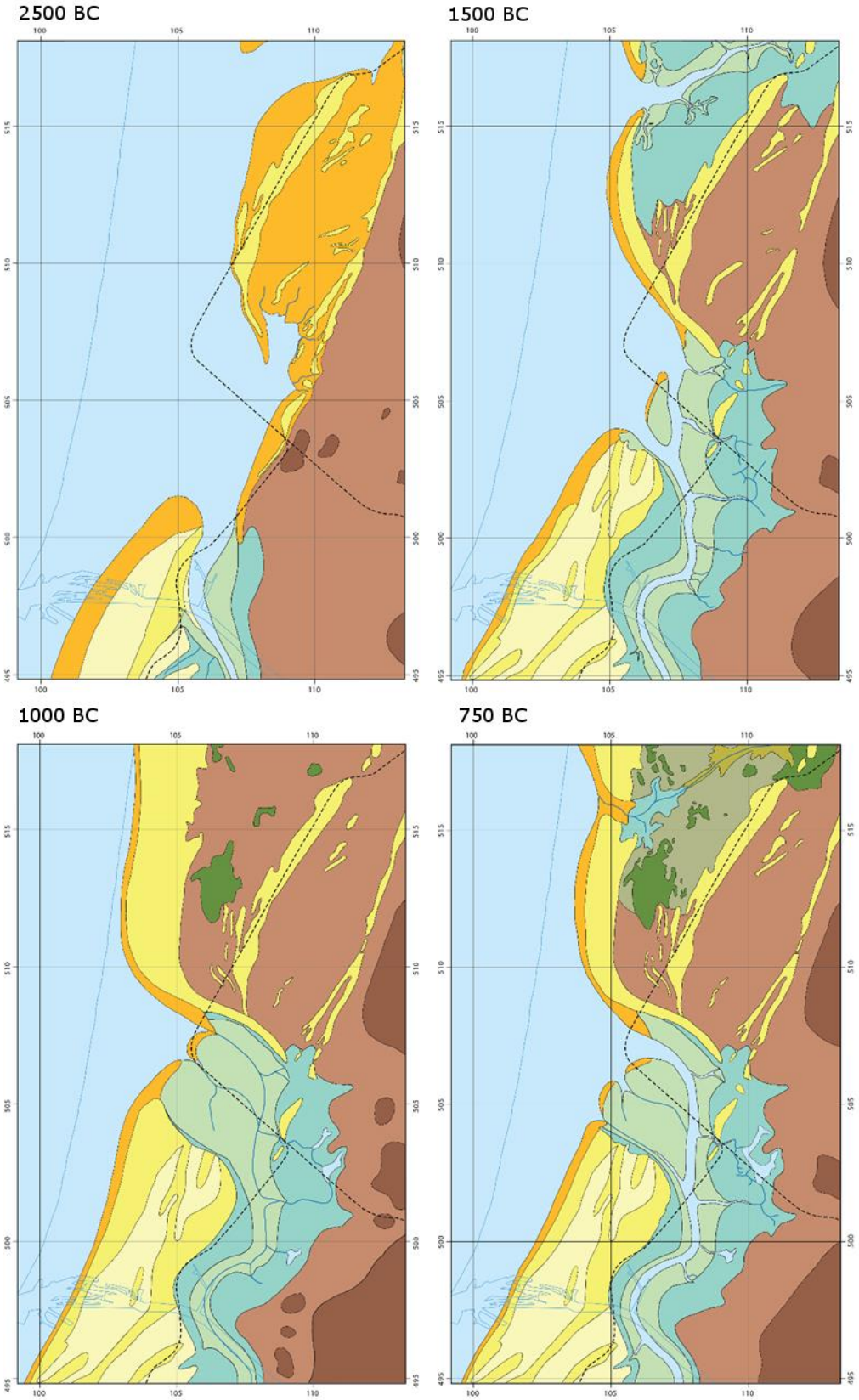

Figure 3: Geologic reconstruction maps of the Oer-IJ estuary (Vos et al. 2010) for 2500 BC, 1500 BC, 1000 BC and 750 BC.

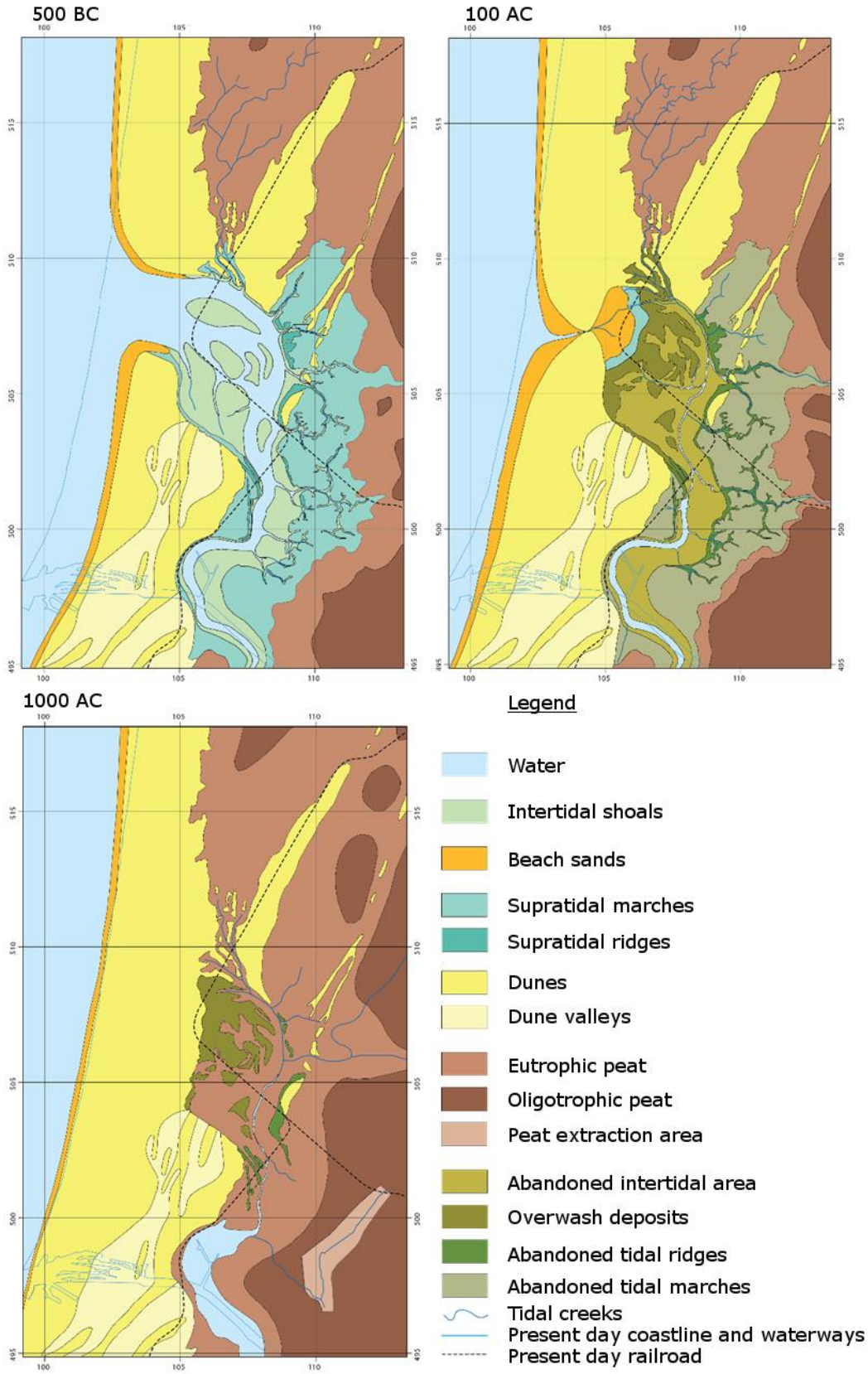

Figure 4: Geologic reconstruction maps of the Oer-IJ estuary (Vos et al. 2010) for 500 BC, 100 AC and 1000 AC along with a corresponding legend.

The Oer-IJ estuary formed when a beach barrier at present day Castricum, 20 kilometer north of the former tidal inlet of Haarlem, was breached and connected with the remnants of this tidal inlet. At Castricum the beach barrier was located further landward compared to surrounding barriers which may have stimulated a higher storm surge at such location. A storm surge is opted to have initiated a breach in the beach barrier. Water, from hinterland peat areas, may have accumulated behind the beach barrier prior to the breach and can stimulate the formation and opening of a new tidal inlet. The opening of the Oer-IJ took place between 3000 BC and 2500 BC. By 2500 BC (Figure 3) the estuary shape was roughly fixed and connected to the hinterland by a channel which used to drain peat areas into the Haarlem tidal inlet.

From 2500 BC onward the estuary was established with estuarine tidal patterns; salt marches on the boundaries and tidal plates in the center of the estuary (Figure 3). In this period the estuary increased in surface area by erosion of the surrounding peat areas. Wind generated waves could traverse further inland due the breach in the beach barrier and erode the peat at the landward side of the estuary. A larger tidal area increases the tidal range and width of the tidal inlet (Stive & Wang 2003) which had a positive feedback on the erosion in the estuary.

Tidal influence increased further around 1500 BC, by then the estuary shape caused the maximum high water level to increase further and enlarge the tidal area even further. Between 1500 and 1000 BC the estuary was active and remained at position despite the progradation of the coastline which occurred in the Late Holocene. From 1000 BC onward (Figure 3) the estuary gradually becomes inactive, which most likely was caused by a decreased high water level (Figure 5). In this period the estuary was filled with sediment while salt marshes and surrounding peat areas tempted to box the estuary in. By 800 BC (Figure 3) the estuary was reduced to a small channel with sparse tidal influence. This channel drained peat areas in the hinterland. At the sea side of the estuary the beach barriers almost closed the estuary off.

Around 650 BC the estuary was reactivated. Most likely the estuary was reactivated by an increased discharge from the hinterland. Coinciding two major water sources were located in the hinterland, the Flevo-Lakes and the Rhine tributary (Hollandse) Vecht that will both be discussed hereafter. After the estuary reopened, marine and tidal processes stimulated erosion and increased tidal area. This increase in tidal area is further stimulated by soil compaction due clay deposition on peat areas. From 550 BC onward the estuary reestablished (Figure 4) and the estuary became a sediment trap. Up to 400 BC the soil compaction was able cope with the sediment deposition, but the estuary started to silt up hereafter. This reduced tidal prism and narrowed tidal creeks and channels, as such it will reduce tidal influence even further. Up to 200 BC a channel remained, though tidal influence was limited and beach barriers started to close off the inlet. After 200 BC the estuary was only under tidal influence during storm surges and eventually wash-over's became the dominant marine process (Figure 4). Nevertheless the area behind the beach barriers was never drained through the Oer-IJ again(Figure 4).

The geologic reconstruction of the estuary between 1000 and 0 BC is partly based on water level reconstruction (Figure 5). Water level is not measured directly but is mainly reconstructed by botanic and archeologic findings along the boundary of the estuary. As a result it is mainly the high water level that is validated, and only specified over the entire estuary, while the low water level is interpretation based on this high water level and estuarine topography like cross-sectional area among others (Vos 2014).

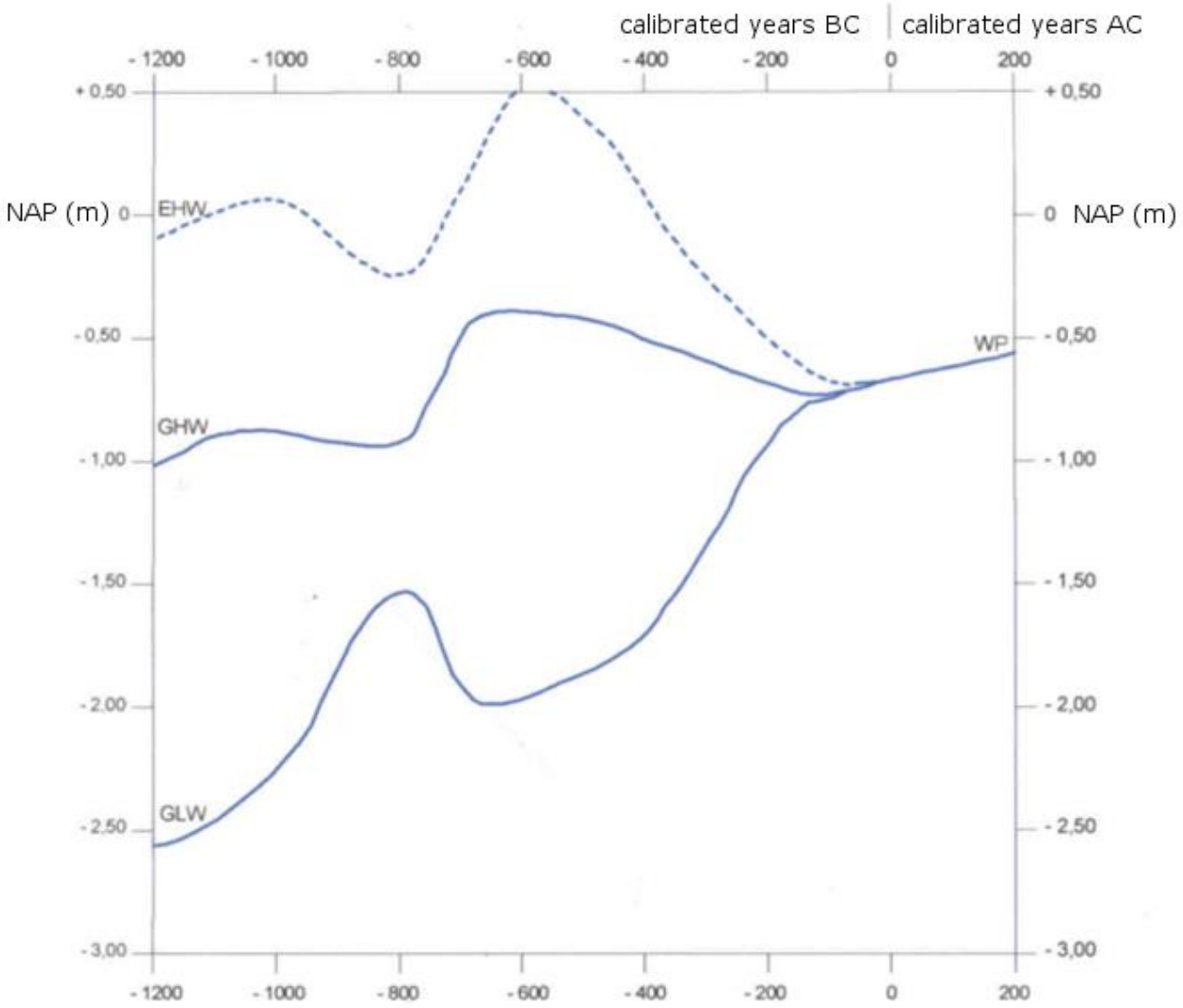

Figure 5: Reconstructed water level curves in the Oer-IJ estuary between 1200 BC and 200 AC for extreme high water (EHW), mean high water (GHW) and mean low water (GLW) against dutch reference height (NAP). WP is the final water level after closure (Vos 2000).

Vecht River

The Angstel-Vecht system was a river system which contained both the Hollandse Vecht (further mentioned as Vecht) and a smaller tributary the Angstel river. This river system was the first tributary of the Rhine which flowed in northern direction. The system was adopted 2970 yr BP (1000-950 BC) and traversed several shallow lakes (Bos et al. 2009). The river system supplied sediment which was captured in these lakes which filled within the period of activity. As a result sediment supply at the downstream part is very limited. River discharge in the period of activity was estimated at 628 m3/s (Bos 2010). Fluvial activity seized about 2270 yr BP (300-250 BC) in the Angstel-Vecht area and was related to channel avulsions which diverged the main Rhine branch to Rotterdam tidal inlet. After these avulsions the Angstel-Vecht river system was mainly used for local drainage.

Flevo-Lakes

The Flevo-lakes consisted of two separate lakes (freshwater lakes in Figure 2) in the former Zuiderzee area. These lakes were so called peat lakes and reconstruction indicate two separate lakes. The southern of the Flevo-Lakes (Almere) was connected to the Oer-IJ estuary by a relative deep and narrow channel through peat areas (Vos et al. 2010). The Vecht river drained at the southern edge of this lake, close to the connection with the Oer-IJ. This lake was no inland sea but had nevertheless an open connection to the sea. Deposits prior to activity of the Vecht show marine deposits at the southern edges of these lakes (Bos et al. 2009). Tidal influence should have reached these areas and caused a tidal range of (several) tens of centimeters in the periods of activity of the Oer-IJ. The Flevo-Lakes were eventually drained to the north, through the Vlie tidal inlet (Vos et al. 2010). This northern breach took place coincidally with the closure of the Oer-IJ. And so the closure of the Oer-IJ estuary is a possible forcing for the opening of the the Vlie inlet in the north or vice versa.

Hypothesis derived from geologic interpretation

This overview coupled with visualized reconstruction (Figure 2-Figure 4) highlights several questions or assumptions. At first the geologic reconstruction indicates two periods of activity separated by a period where the estuary was almost closed off. This assumption is based on a severe reduction in tidal range over this period (Figure 5). The reconstruction couples the reactivation with an increased river discharge, nevertheless research showed the Vecht river was already active (Bos et al. 2009) in the period the estuary was almost closed off between two periods of activity. Moreover the reconstruction couples the final closure to the lack of river discharge due other flow paths in the Netherlands.

Figure 6: Andersons tidal inlet, Victoria, Australia (Google Earth).

Moreover the Oer-IJ estuary shows a characteristic shape; the sharp bend directly landward of the estuary mouth is often unusual in present day estuaries. Exceptions exist (Figure 6) but are very limited and barely studied. The meandering continuation after the first bend is less unusual but the effect of these sharp meandering bends is not well studied within estuarine environments. In particular modelling studies tend

to generate simplified estuaries (Hibma et al. 2003; Van der Wegen et al. 2010; Robins & Davies 2010) as the effect of minor bends are limited compared to error margins or uncertainties of numerical modelling. Nevertheless sharp bends in rivers are better studied and suggest hydro and morphodynamics are altered when bends become too sharp (Blanckaert et al. 2013). Estuarine environments differ naturally from rivers due the bidirectional flow, but the effects of sharper bends is an uncertainty as of yet.

Finally the reconstruction indicate several bars in the outer part of the estuary, as well as several tidal creeks at the boundaries of the estuary. In particular these bars are interpretation, these bars are not recorded in any geologic record but are implemented to both reduce estuary size based on present day estuarine bar pattern knowledge.

Hypothesis

Considering these interpretations of the geologic reconstruction of the Oer-IJ several question remained. Answering these questions will tend to improve the reconstruction.

As first question this study will look what the effect is of river discharge on estuarine bar pattern. It is expected that river discharge has impact on the estuary as an decreased river discharge is assumed to have closed the estuary (Vos et al. 2010).

Secondly this study will look at what the effect of estuarine shape is on estuarine bar pattern. Modelling studies often used simplified straight grids, but river morphology studies have shown the effect of bends on river and bar morphology. It is expected some bars will become fixed due bends in the estuaries while others may propagate as free bars.

Finally we will look what the effect of other parameters is on the estuarine bar pattern. Several modelling parameters have been introduced (Lesser et al. 2004) as dominant in modelling studies as such it is expected some of these parameters can influence the bar pattern in estuaries heavily.

Self-evident the study will try to couple the research questions to the geologic reconstruction.

Methodology

The main research questions will be handled by a modelling study in Delft3d (Lesser et al. 2004). For this study only the FLOW module (including MOR and SED modules) will be used, the WAVE module and other Delft3d modules will be neglected. All model runs are run in a window of a month under similar circumstances. Each run is run as one computation. Several model runs that were interrupted due technical breakdowns, these runs were restart on their last map file, show no sign of their interruption. The version used in this modelling study is the 4.00.02 version of Delft3d.

The set-up of the model is only based on the geologic reconstruction map. Several Delft3d models (Teske 2013) were used to fine tune some boundary conditions and parameters. The models uses a depth-averaged approach. The results of this study consist of model runs for 22 different scenarios, an overview of these scenarios is given in Table 1 and each variable will be discussed individually.

Table 1: Overview of all used model runs with information of variables (enclosure shape, river discharge, alfabn parameter, tidal components and initial bathymetry. [a] 310O has a linear decrease in discharge, 311O has a sudden decrease in discharge. [b] idealized trumpet shape bathymetry is similar to Oer-IJ bathymetry in elevation, the coordinates differ naturally.

Model nr.	Enclosure shape	River discharge	Alfabn	tidal components	Bathymetry
300O	Oer-IJ	180	10	O1, M2, M4	a180
301O	Oer-IJ	90	10	O1, M2, M4	a90
302O	Oer-IJ	540	10	O1, M2, M4	a540
303O	Oer-IJ	360	10	O1, M2, M4	a360
304O	Oer-IJ	180	10	M2, M4	a180
305O	Oer-IJ	180	10	O1, M2	a180
306O	Oer-IJ	180	10	M2	a180
307O	Oer-IJ	180	1	O1, M2, M4	a180
308O	Oer-IJ	180	100	O1, M2, M4	a180
309O	Oer-IJ	0	10	O1, M2, M4	a180
310O	Oer-IJ	180->0[a]	10	O1, M2, M4	a180
311O	Oer-IJ	180->0[a]	10	O1, M2, M4	a180
300S	Straightened	180	10	O1, M2, M4	s180
301S	Straightened	90	10	O1, M2, M4	s90
302S	Straightened	540	10	O1, M2, M4	s540
303S	Straightened	360	10	O1, M2, M4	s360
309S	Straightened	0	10	O1, M2, M4	s180
300T	Trumpet	180	10	O1, M2, M4	t180=a180[b]
301T	Trumpet	90	10	O1, M2, M4	t90=a90[b]
302T	Trumpet	540	10	O1, M2, M4	t540=a540[b]
303T	Trumpet	360	10	O1, M2, M4	t360=a360[b]
309T	Trumpet	0	10	O1, M2, M4	t180=a180[b]

Model domain and grid

The initial model set-up is based on the geologic reconstruction of Peter Vos. In this reconstruction the time slice of 500 BC is used as reference for the model. This time slice (Figure 7B) visualizes the estuary

just after the reactivation in 600 BC. According the reconstruction the estuary will be inactive within 400 years. From this reconstruction map the channel and intertidal areas are included as well the beach area. The model exclude supratidal area (marshes) as well tidal creeks which are located within the marshes. This combined area was used as the landward enclosure for our model (Figure 7). The sea basin is enclosed by north and south boundaries of roughly 10 km perpendicular to the local coastline. The seaward boundary (west) is intended to be as parallel to the coastline as possible. The expansion of the estuary landward of the known boundaries was done with a long regular bend that turns eventually in a long straight end up to a distance of 45 km from the mouth of the estuary. The width of the estuary resembles the intertidal area in the geologic reconstruction. For the upstream part the width converged linear with 50m/km until a fixed width of 200 m was reached. Grid boundaries were slightly altered to decrease sharp corners which tend to focus erosion disproportional.

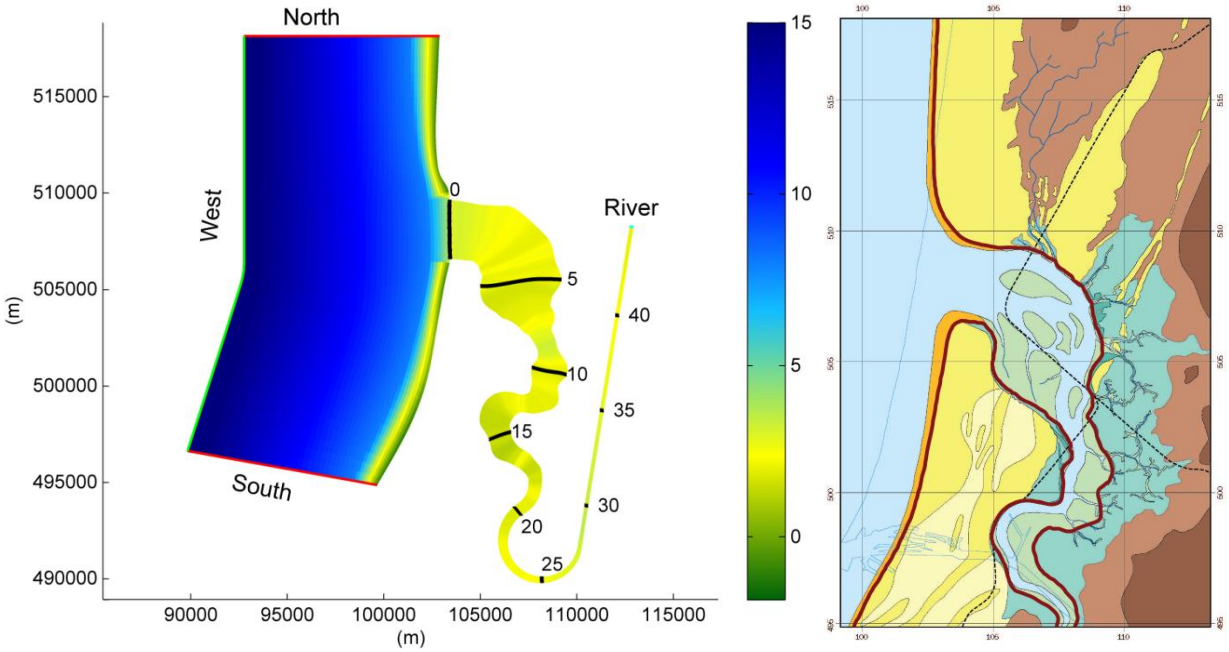

Figure 7: A) Model grid with initial bathymetry of the default scenario, four open boundaries (North, West, South and River) and distance to the mouth if the estuary. B) Geologic reconstruction of the area at 500 BC (Vos et al. 2010) *with red lines indicate the boundary of the modelled grid.*

Within the enclosure a curvilinear grid was made with RGFGRID. Over the entire estuary the grid is 36 grid cells wide, the width of each cell thus resembles 1/36 of the width of the estuary at a location, in a range from 6 meter up to 125 meter. The length of each grid cell in the center of the estuary is roughly equal in the midline of the estuary and in the order of 50 meter. This set up generates in particular elongated cells at the inland section of the model, as well slightly wide cells at the areas with the largest width in the estuary. In contrast the cells in the central part of the estuary become most square. The elongated cells at the inland part of the model are not expected to dominate the model as flow direction in these section is predominant parallel to the cell length. At the sea basin cell size differs, cell width increases from 80 up to 500 m the further away from the mouth (northern and southern direction) while cell length increase from 50 m to 500 m the further away from the coastline. After generation the grid was slightly orthogonalized

three times in standard settings to optimize continuous flow. Initial test runs were done on a coarser grid with grid cells that had double width and length.

Bathymetry

The initial bathymetry is composed by a multi-step approach. At first bathymetry for coarser grid runs was investigated. Several variations of bathymetry were tested, including rectangular flat bed, v-shaped channel as well as different variations of general elevation and bed level slope along the entire estuary. These coarser models ran under similar settings for 1 year. Out of these models the model with an initial rectangular flat bed with a water depth of 4 meter at the mouth and 2 meter at the river boundary with an uniform slope was chosen. This choice was primarily based on how much infilling had occurred. From this model the final bathymetry was chosen. This bathymetry was averaged over width for each row of cells perpendicular to the centerline. The result, a vector with average depth as a function of distance from the mouth of the estuary along the centerline, was used to interpolate an initial bathymetry for the finer grid model runs. As a result the initial bed level elevation is similar over the width of the estuary but varies over the length of the estuary, both increasing and decreasing. This method results in initial bed levels which are closer to the final bed level, thereby reducing the time the model has to run, in particular as sediment transport is limited as seen later. This method has been applied for all combinations of shape and river discharge, except 0 m^3/s river discharge. As a result the 0 m^3/s river discharge bathymetry is similar to the 90 m^3/s river discharge bathymetry.

Bathymetry at sea is fixed and does not differ between scenarios, it decreases linear from 15 meter depth at the seaward boundary up to 8 meter at roughly 3 km of the coastline. Hereafter depth decreases linearly to -2 meter at the coastline. At the outflow of the estuary, bathymetry was determined as the maximum depth out of estuarine bathymetry and the sea basin bathymetry, to generate a free outflow for the estuary (Figure 7A).

Table 2 Harmonic components used at the seaward boundary of the model.

Component	Frequency (deg/h)	Amplitude begin (m)	Phase begin (deg)	Amplitude end (m)	Phase end (deg)
O1	13.9438	0.11	7.4023	0.11	0
M2	29.0323	0.66	15.4123	0.66	0
M4	58.0645	0.17	30.8246	0.17	0

Boundaries

The model consist of four open boundaries, three located at the sea basin and one located at the upstream part of the model to resemble river input (Figure 7). The upstream 'River' boundary is prescribed as a 'discharge per cell' boundary. This boundary consist of 18 individual boundaries of two cells each, each cell taking 1/36 of the total discharge. This type of upstream boundary generates a stable canal type of outflow where the upstream boundary is not influenced by downstream perturbations.

The three open boundaries around the sea basin are used to prescribe the propagating tidal motion along the coast in the area. Three harmonic components are used within this study, M2, M4 and O1 (Table 2). These components are computed by harmonic analysis on present water level data at IJmuiden (**live**.**waterbase**.nl/), which is located roughly at the southern boundary of the model. The western boundary is a water level boundary with harmonic forcing. Along the boundary a constant amplitude is used combined with a phase difference based on the length of the boundary and frequency of each of the

components. The northern and southern boundaries are based on water level gradients, so called Neumann boundaries. In combination with an harmonic water level boundary at the seaward side, the tide and tide induced water motions propagate correctly along the coast (Roelvink & Walstra 2004).

Timeframe

All models had a time step of 12 seconds, which leads to a Courant number < 10 in the main area of interest. The maximum was only violated in the straight upstream part of the model. As water motion here is predominant in longitudinal direction, slightly increased Courant number due to grid size in transverse direction can be neglected. Other areas of the model were not violated.

The morphological time scale factor (morfac) was set at 400, which indicates that all erosion and deposition in each time step is multiplied by 400. Morfac values of 50, 100, 200 have been investigated but morphologic differences in final bathymetry between a morfac of 50 and 400 were minor and could not compensate the decrease in run time. These findings correlate with other modelling studies (van der Wegen 2013; Ranasinghe et al. 2011).

All model runs ran over 369 hydrodynamic days, which resembles 403 morphologic years. To limit run time model map output was given roughly every 4¼ tidal cycle of the main tidal component M2. A second type of run is introduced to gather more detailed information of water level data in the final estuary. This run type generates no morphologic change but give map output every 12 minutes over a period of 4 days, these type of runs are done for all the different models and are hereafter mentioned as 'hydrodynamic runs'. These hydrodynamic runs have the last output map of the main run as initial condition and have identical parameters as the main runs only with an increased map output (every 10 minutes). These runs are expected to give detailed information of the location of intertidal cells in the area.

Sediment

Non-cohesive fine sand (200 µm) with a density of 2650 kg/m^3 is used as sediment in all runs. A sediment size which correlates with geologic cores that found grain sizes of 150-215 µm (Vos 2012; Vos et al. 2010). The bed consist of one 30 meter thick layer of this sediment, a bed which is never entirely penetrated in a model run.

Sediment transport is not prescribed at any of the boundaries, despite equilibrium sand concentration profile is used at the inflow boundaries. This causes sediment concentrations at the inflow boundaries equal to the maximum transport capacity at that location at a certain time (Deltares 2011), thereby it maintains the bed level at the inflow boundary and will stabilize the inflow.

Engelund-Hansen sediment predictor (EH) (Engelund & Hansen 1967) is used as sediment predictor in the models. EH is favored over Van Rijn (1993) sediment predictor (van Rijn 1993) mainly due the deep narrow channels that the Van Rijn sediment predictor generated in particular on the side of the estuary, channels with transverse gradients out of order with the angle of repose for non-cohesive sediment.

Model parameters

Transverse bed slope effects are incorporated in two important model parameters, the Ashld parameter (Koch & Flokstra 1980) and the AlfaBn parameter (van Rijn 2007). AlfaBn is the main parameter that introduces transverse bed slope effects into the model:

$$S_{b,n} = |S_b'|\alpha_{bn}\frac{\tau_{b,cr}}{|\vec{\tau}_b|}\frac{\delta z_b}{\delta n}$$

wherein $S_{b,n}$ is the additional bed-load transport vector in direction normal to the unadjusted bed-load transport vector, $|S_b'|$ is the magnitude of the unadjusted bed-load transport vector, α_{bn} is the user defined parameter, $\tau_{b,cr}$ is the critical bed shear stress, $|\vec{\tau}_b|$ is the bed shear stress due to currents and $\frac{\delta z_b}{\delta n}$ is the bed slope in direction normal to the unadjusted bed-load transport vector (Deltares 2011). Ashld parameter is an additional parameter which alters the weighting of angle θ in the transverse bed slope computation:

$$\tan(\phi_s) = \frac{\sin(\phi_\tau) + \frac{1}{A_{sh} f(\theta)} \frac{\delta z_b}{\delta y}}{\cos(\phi_\tau) + \frac{1}{A_{sh} f(\theta)} \frac{\delta z_b}{\delta x}}$$

wherein ϕ_τ is the original direction of the sediment transport ϕ_s is the final direction of sediment transport , $\frac{\delta z_b}{\delta x}$ and $\frac{\delta z_b}{\delta y}$ are the bed slope in x and y direction respectively, $f(\theta)$ is a function of the Shields parameter and A_{sh} is the Ashld tuning coefficient optionally specified by the user (Deltares 2011).
Both parameters were varied in the optimization of the model. Ashld was found to be of limited effect compared to AlfaBn, therefore AlfaBn is used as a variable further in this study. Fixed values of AlfaBn (10) and Ashld (1) were used in the reference model of this research.
The model starts with an initial uniform Chézy bed roughness coefficient of 65 $m^{0.5}/s$. A bedform roughness predictor (van Rijn 2007) is used in the model following previous modelling studies on tidal basins (Teske 2013). Each time step the predictor computes a roughness height (k_s) for dunes, mega-ripples and ripples at each cell. The combined bedform height (k_s) is then used to compute the roughness in the cell at each time step and overwrites the previous roughness.
Secondary flow implements the effect which is known as helical flow in rivers into 2D models (Kalkwijk & Booij 1986). Helical flow, the effect where water movement is directed to the outer bend near the water surface and to the inner bend near the water bed, is a well-known effect in river bends. In estuarine modelling the effect of secondary flow is small (Coeveld 2002). Nevertheless this study shall not neglect this flow as in particular in the Oer-IJ estuary several relative sharp bends exist where, in particular compared to previous modelling studies, it is assumed helical flow is significant in these bends.

Excluded parameters.

The model runs are calibrated to several parameters, nevertheless many aspects of a realistic estuary are neglected, both to prevent complexity due interconnectivity of parameters, to focus on the main variables of research and to keep model running and building time within bounds. All model runs are excluded from wind and wave influence as well excluded from wind and wave generated currents.

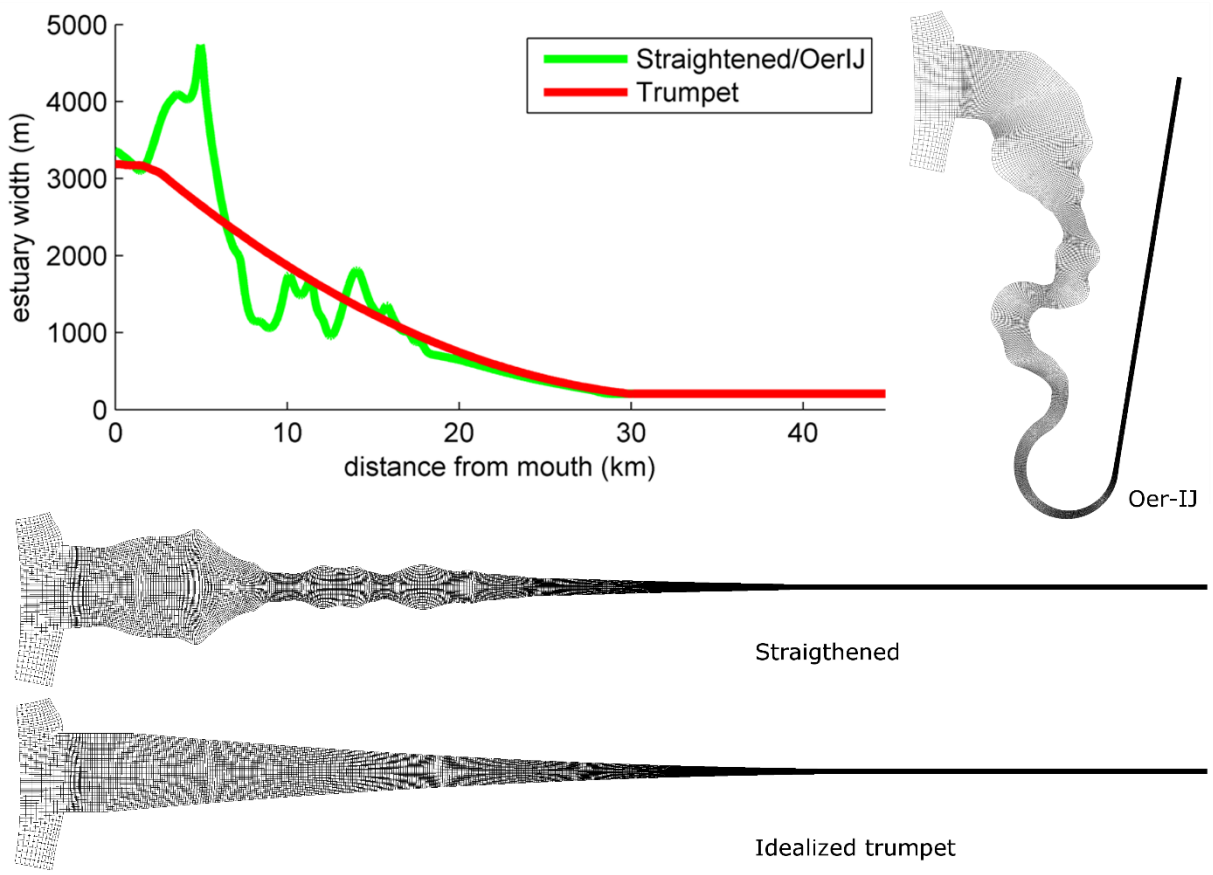

Figure 8: Estuary width as function of distance from the mouth for the Oer-IJ, straightened and idealized trumpet grid shapes together with three grids (without basin area) for the three different shapes.

Grid shapes

The Oer-IJ estuary model is compared with two different grids to estimate the effect of the topographic forcing of the bended estuary (Figure 8). The first grid, hereafter mentioned as 'Straightened', is a straightened version of the Oer-IJ grid. In this grid the midline of the original grid is straightened and width at each point is determined by the width of the original estuary. The second grid, hereafter mentioned as 'Idealized trumpet', resembles the shape of a trumpet. The width at the mouth of the estuary is similar to the mouth in the original grid and the width at the upper non-convergent part is similar to the original too. In between the width is based on the best fit of a 2nd order polynomial function (Figure 8). Both grid shapes are preprocessed like the original grid.

River discharge

River discharge is was varied in several model runs. Models are run with a constant river discharge of 0, 90, 180, 360 and 540 m^3/s . The maximum river discharge used in our models, 540 m^3/s, is comparable with the discharge in the main activity period of the Hollandse Vecht river (Bos 2010). Peak flood discharge during floods is neglected in this model as it is both uncertain due to buffering by the Almere lake and smaller lakes in the lower Vecht area and complex to include upstream water level and discharge

variations. All five discharges are run on the three different grid shapes in order to compare the combination of the two main variable parameters of this study too.
In order to model a gradually decrease of Vecht discharge, as an example of a diminishing discharge due a gradual shift in the division of discharge upstream between the Vecht river and other branches of the Rhine river (Bos et al. 2009), one model run consist of a linear decrease in discharge over time. The initial discharge equals 180 m^3/s and linear decreases to 0 m^3/s after 369 hydrodynamic days, the end of the model run (Figure 9). Another model (Figure 9) consist of a sudden decrease in discharge. The first 6 hydrodynamic months is constant at 180 m^3/s, thereafter the discharge decreases linear from 180 m^3/s to 0 m^3/s in one hydrodynamic month. The last 5 months of the model the discharge is kept constant at 0 m^3/s. This model run is done to model a sudden stop of discharge of the Vecht river, either by a sudden avulsion in the Rhine river or the connection to the Vlie inlet (Vos et al. 2010). Both temporal variations in discharge are only done for the Oer-IJ shape. River discharge is fixed at 180 m^3/s in the remaining model runs.

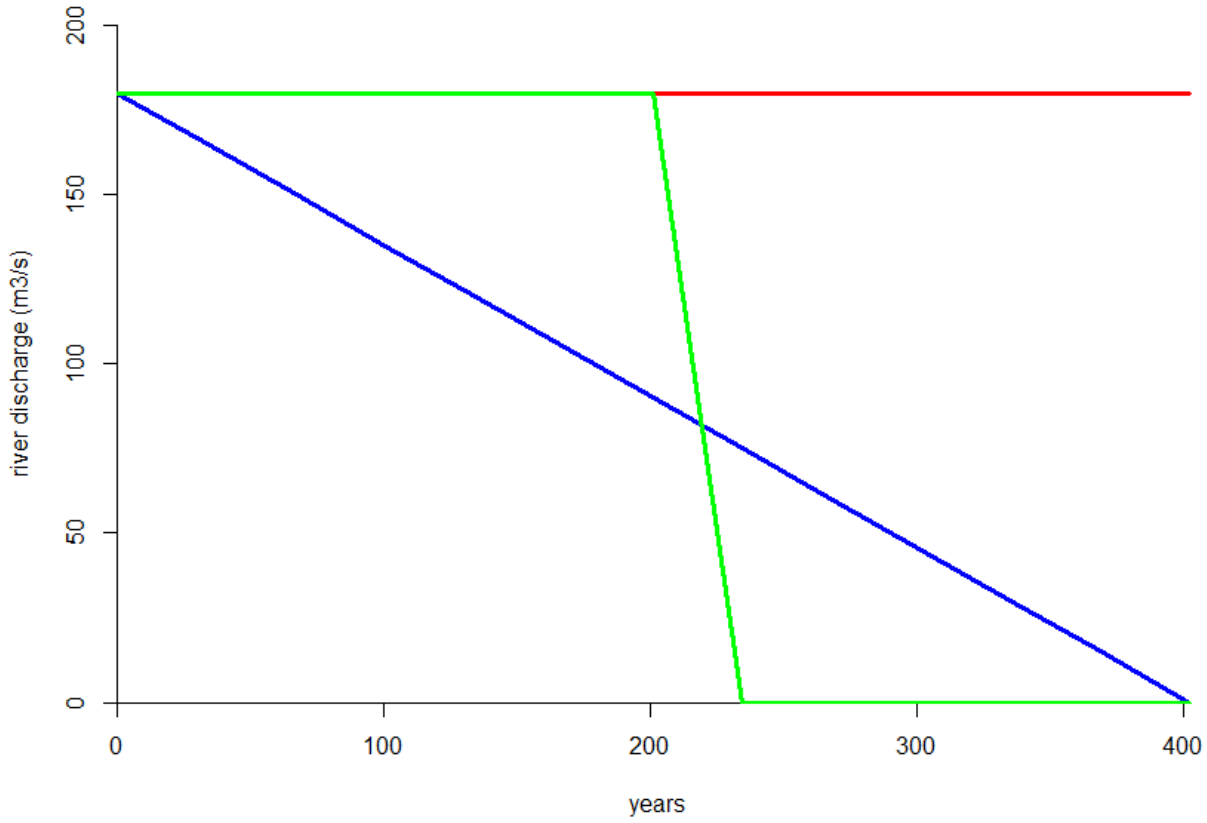

Figure 9: Different discharge regimes used in the variable discharge models. Colors indicate reference model of 180m^3/s (red), linear decrease (blue) and sudden decrease (green).

Tidal components

Variations on the sea boundaries is done in four model runs. For the model the tidal components M2, M4 and O1 are used (Table 2). Four model runs are done to investigate the influence of each tidal component and to validate that the morphology is not predominant determined by these tidal components. The four

runs use the following combination of tidal components; M2 + M4 + O1, M2 + M4, M2 + O1 and M2 only. This comparison will be done only for the Oer-IJ grid shape.

Alfabn

This transverse bed slope parameter turned out to be the most dominant in preliminary coarser grid runs. As such this parameter was chosen to be variable in three model runs to validate that morphology is not predominant determined by this AlfaBn parameter. The fixed value chosen for all model runs equals 10, in the variation values were chosen an order of 10 higher and lower at 1 and 100. Like other minor variable parameters, AlfaBn variation will only be done on the Oer-IJ grid shape.

Results

The 22 different scenarios used in this modelling study all show similar results. Figure 10 shows final bed level elevation (after 404 years) for a high (540 m^3/s) and a low (90 m^3/s) discharge in both the Oer-IJ scenario, the straightened scenario and the idealized trumpet scenario. In all scenarios multiple channels are located at the mouth of the estuary, inside the estuary they form a braided pattern of channels and bars. The number of these parallel channels decreases in landward direction towards a single channel which eventually covers either the entire confined estuary width or has regular adjacent alternating bars within the confined area. The maximum bed level elevation increases in landward direction and reaches a maximum elevation 15 to 20 kilometer distance from the mouth. Further landward maximum bed level elevation decreases again.

In the Oer-IJ scenarios (Figure 10, upper figures) several characteristics can be noticed. The most pronounced channel is quite often located at the inner bend of the estuary, the outer bend is most often more elevated and sometimes a smaller channel is located in the outer bend. Nevertheless differences between the high and low discharge scenarios are clearly visible. Both scenarios have multiple channels at the mouth followed by a braided network, however the braided network Is more pronounced in the low discharge scenario. In this scenario a single channel is only reached after roughly 15 kilometer, while the braided network stops to exist already after roughly 10 kilometer in the high discharge scenario. This single channel is also larger in the low discharge scenario. Apart from channel pattern the most pronounced difference is seen in the overall bed level elevation. In the low discharge scenario the most elevated area is both lower and located closer to the mouth compared to the high discharge scenario.

The straightened scenarios of the Oer-IJ (Figure 10, center figures) display similar though slightly altered characteristics for high and low discharge scenarios. However several remarkable differences are clearly displayed too. Like the Oer-IJ scenarios the straightened scenarios the braided network disappears closer to the mouth in the high discharge scenario compared to the low discharge scenario. However a single channel exist closer to the mouth then in the Oer-IJ scenario, particular in the high discharge scenario where a single channel already exist at 5 kilometer from the mouth. The trend in bed level elevation is also similar to the Oer-IJ scenarios, however this trend is more pronounced. In the high discharge straightened scenario the overall bed level elevation of the estuary is higher compared to the Oer-IJ scenario for a similar discharge. In the low discharge scenario this is less pronounced but bed level elevation is nevertheless higher. Finally the location of the most pronounced channel is more centered although a somewhat meander like pattern still exists. The bends at the river side of the estuary (10 to 20 km from the mouth) are sharp. These bends are not only sharper than the confined shape of the Oer-IJ but also sharper than the channel bends imposed by the curved confined shape of the Oer-IJ.

The results of the idealized trumpet scenarios (Figure 10, lower figures) resemble the straightened scenarios better compared to Oer-IJ scenarios. The bed level elevation along the entire estuary is almost similar as the general bed level elevation in the straightened scenarios for both the high and low discharge scenarios. However channel pattern differs slightly between these scenarios. The braiding network extends quite far inland, although the number of channels is reduced more gradual compared to the other scenarios. Moreover a single channel is reached not before just over 15 kilometer from the mouth. The major difference with other scenarios is definitely the symmetry in these scenarios, the pattern is far more constant over width compared to the other scenarios. In particular in these idealized scenarios there is the

difference in extension of the estuary into sea, it propagates far into sea with high discharge and less far in low discharge, a difference which is more pronounced compared to the other scenarios.

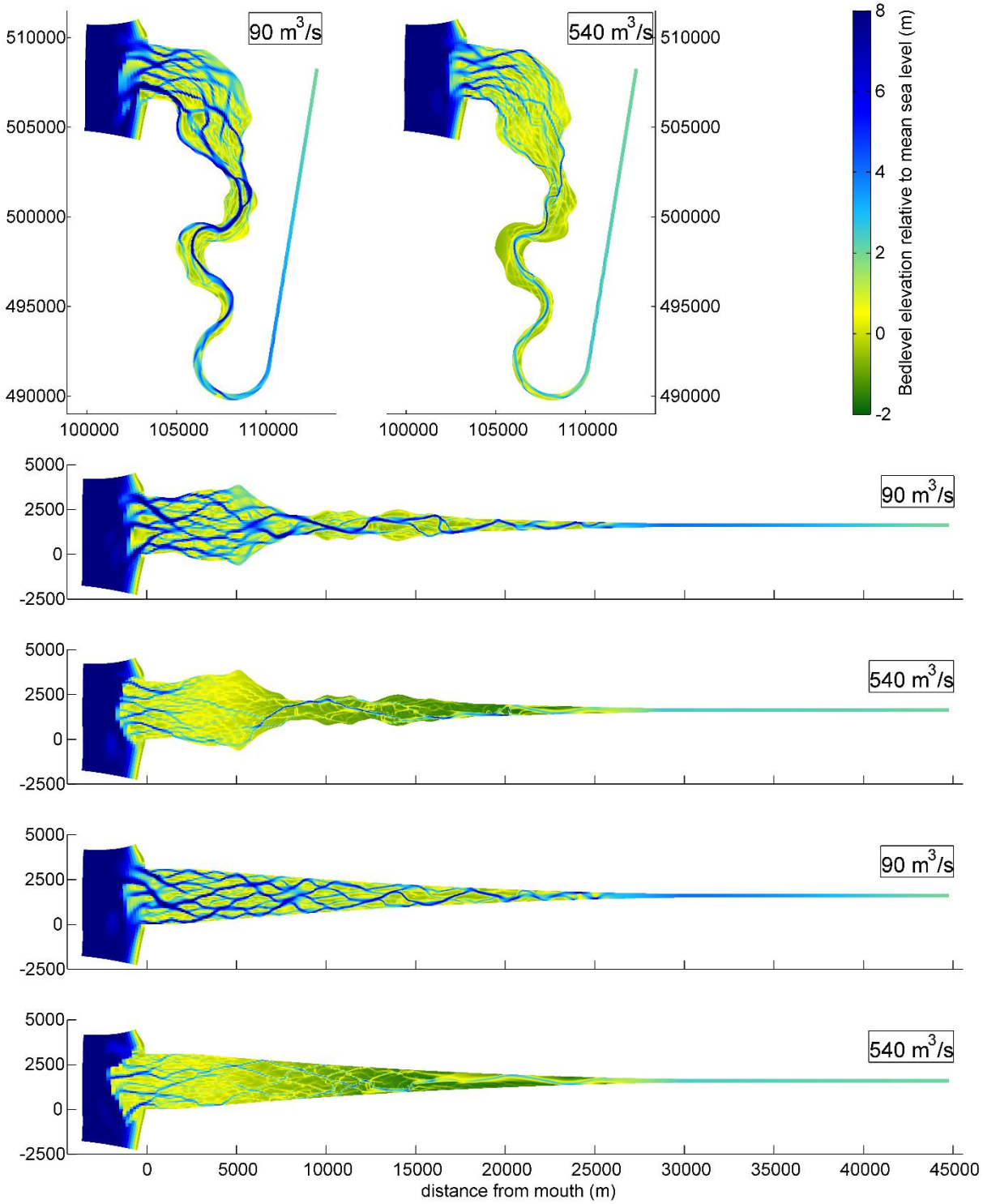

Figure 10: Overview of final bed level elevation for low and high river discharge for Oer-IJ, straightened and idealized trumpet shape scenarios.

Overall these results display that a higher river discharge causes a higher elevated estuary with less channels, channels that are also slightly smaller, and a braided pattern which extends less far landward compared to lower river discharge. The effect of shape is most pronounced by the location of the channel that prefers the inner bend in the Oer-IJ scenarios and the more symmetric behavior in the idealized scenarios. Nevertheless the braided behavior visible in all scenario is very dominant in the estuarine morphology within the models.

Stability of the estuary over time

Final bed level elevation maps are used within this study as the primary result. However these maps are only gathered at one specific time. As a result these maps lack the information if the channel pattern is stable or dynamic as well whether the estuary itself is in equilibrium or still progressing towards another state. An overview of bed level elevation at multiple time steps will be used as an indication on how well the final bed level maps are representative for long term (Figure 11Figure 1).

The first row of figures show the estuary over time with a constant discharge of 180 m^3/s. The estuary is subject to rapid infilling, after 100 years the entire upper part of the estuary has an already characterized pattern, while the majority of the lower part consist of bars and channels too. After 200 years only the outer bend of the first bend of the estuary is not yet well formed, this outer bend only forms relative slow as after 400 years the outer bend was just filled up. The general pattern of bars and channels in the estuary is relative stable, channels migrate slightly but the pattern remains very similar after an initial pattern was formed. Most of the morphology is already stable after 200 years.

The second row (Figure 11) displays the time series of a linear decrease in river discharge over time. Linear decrease from 180 m^3/s at 0 year to 0 m^3/s at 400 year (Figure 9). After 100 years the model results are almost identical to the case with constant river discharge, differences at further time steps increase but are still minor. Nevertheless the morphology in the outer bend of the first bend forms slower in the decreased discharge scenario, in particular in the second half of the model runtime. Moreover the channels seem to become more stable in this scenario compared to the constant discharge scenario, in particular in the upper part of the estuary channel are almost stable while channels still alter slightly in the constant discharge scenario.

In the third row (Figure 11) the river discharge has been decreased more sudden. After 200 years the river discharge decreases linear from 180 m^3/s towards no discharge over a period of roughly 30 years. The last 170 years no river discharge is implemented in this model (Figure 9). The sudden change in discharge after 200 years results in minor changes. Small differences exist in the central part of the estuary, here bars either have more area or are cut by minor channels. Moreover channels in particular the central part of the estuary are more pronounced. The final bed level is less dynamic without river discharge and primarily stimulates the morphology formed by the higher discharge. An effect similar to the later phase in the linear decreased discharge scenario.
has an effect though very minimal for at least the window of discharges used. The reduction of discharge within a model run tends to stimulate a less dynamic system without any shift in general channel and bar pattern.

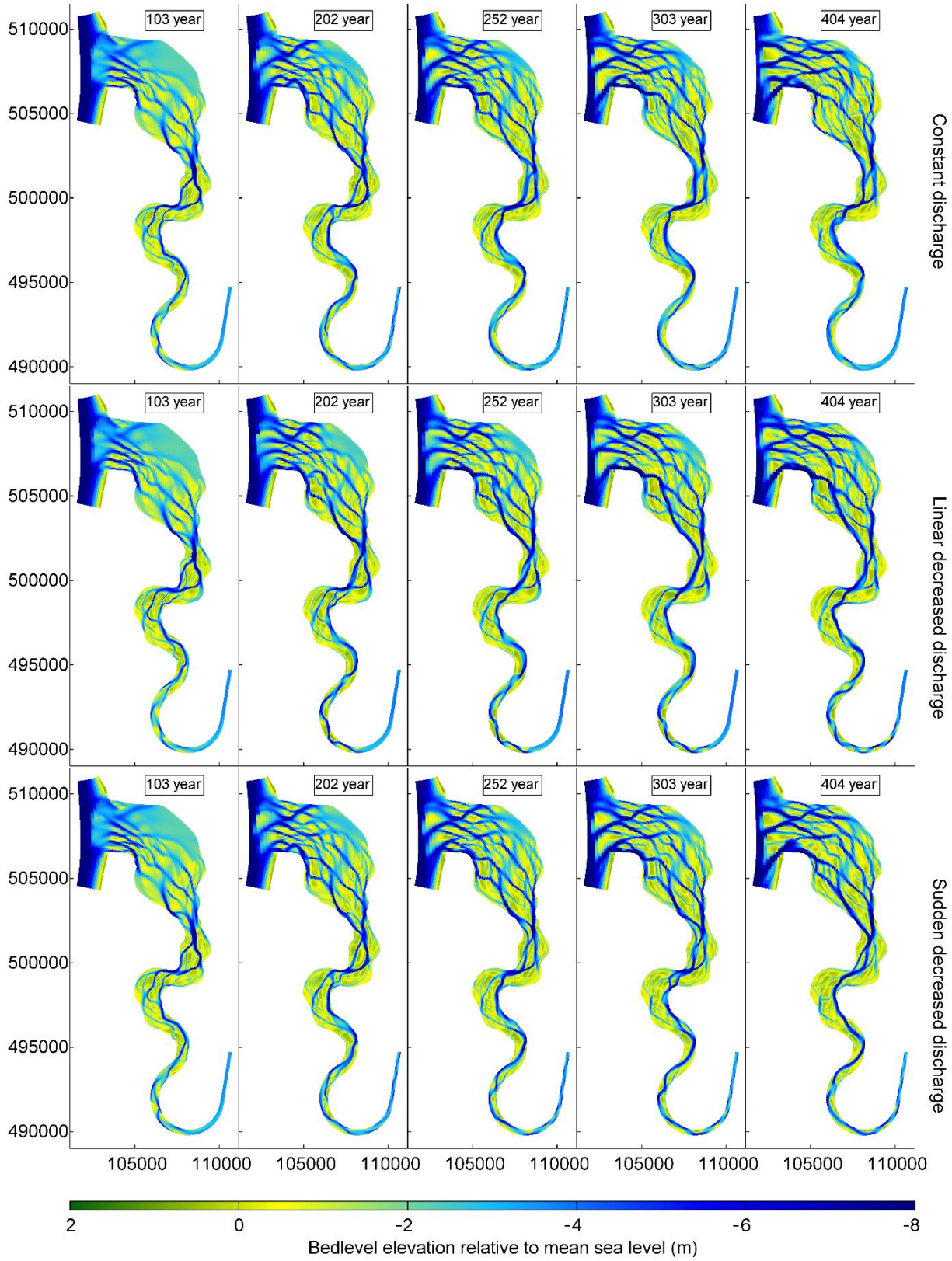

Figure 11: Bed level elevation as time series for a constant river discharge (upper row), a linear decreasing river discharge (middle row) and a sudden decreased river discharge (lower row). Timeslices are set at a period of roughly 100 year and include a 250 year step.

Overall bed level is relative stable, the system is dynamic but the general patterns remain similar over the last 200 years. Therefore it is assumed that the system is more or less in equilibrium after 400 years despite no model runs were done for extended time due to run time limitation. As such the final model runs are representative for each of the specific scenarios. Next to that the effect of either a sudden or a linear decrease

Bed level patterns

Figure 10 presents a selection of the different model runs, despite these maps keep true angles and dimensions it is hard to compare different confined shapes. In this section bed level elevation is presented for each individual cell (Figure 12 and Figure 13) such that different shapes can be compared on pattern. In these figures the cell width is a function of the total width at a distance from the mouth:

$$y^* = \frac{y}{B(x)}$$

wherein y^* is the width represented for one cell in the graph y is the original cell width and $B(x)$ is the total width at a distance from the mouth. As such width of patterns in these figures should not be used quantitatively. Distances are given as distance to the mouth of the initial estuary, all scenarios show bars extend seaward of the former estuary mouth too. Estuary width is variable along the estuary, as such no value should be taken on width of patterns in these figures. Cells do not vary in length at the centerline of the estuary and as such are representative for distance from the mouth of the estuary. In all scenarios bars extend also seaward of the former estuary mouth. Figure 12 compares the three different shapes for different river discharges. Figure 13 shows the results of the Oer-IJ shape with 180 m^3/s river discharge only however in these runs other variables are varied.

River discharge effect on bed level elevation patterns

River discharge is increased in the first five subfigures of Figure 12, these scenarios all ran the Oer-IJ shape. Channel area is more abundant in the lower river discharge scenarios and bed level is more elevated with higher river discharge. All scenarios have a braided pattern the first 5-7 kilometers and are all dominated by 1 main channel at 10 kilometer, 360 m^3/s contradicts as two larger channels coexist up to almost 15 kilometer. In particular the no river discharge scenario has alternate bars, in this scenario alternate bars exist from roughly 10 kilometer where bar length decreases landward. Alternate bars are less pronounced in the lower river discharge scenarios but are pronounced in the high river discharge scenarios. Overall bar pattern is roughly constant from 25 kilometer landward, though bar height still decreases in landward direction. In the central part of the estuary (8-20 kilometer) bends are sharper at lower river discharges and more elongated at higher river discharges. Moreover channels are more elevated and slightly narrower with increased river discharge. These results corresponds with the earlier map views (Figure 10) regarding increased bed level elevation at higher river discharges. Remarkable is that the 180 m^3/s river discharge bar pattern extends least far landward of the five scenarios.

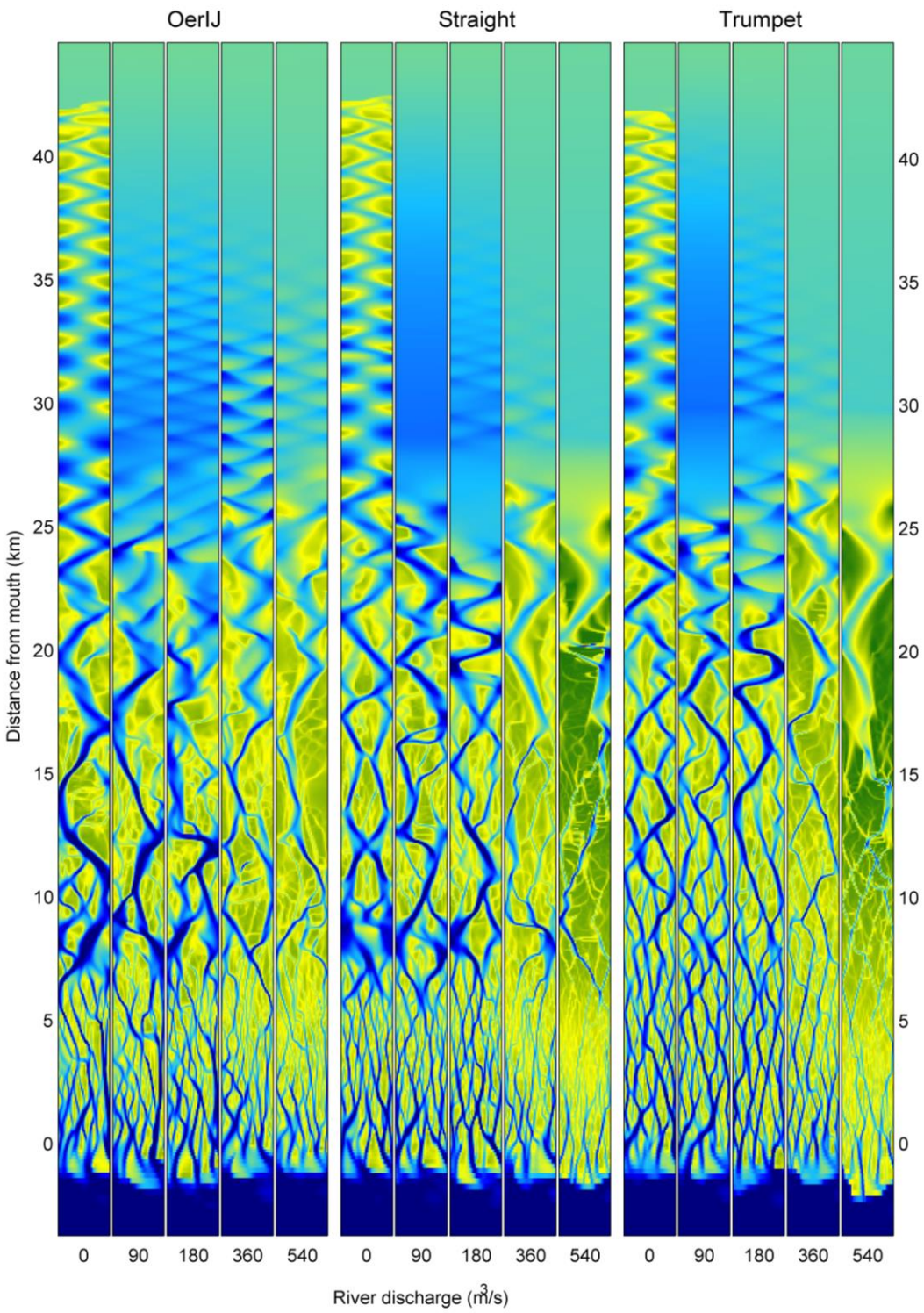

Figure 12: Bed level elevation for distance from estuary mouth against cells that contain the estuary for model runs that vary in river discharge and estuary shape.

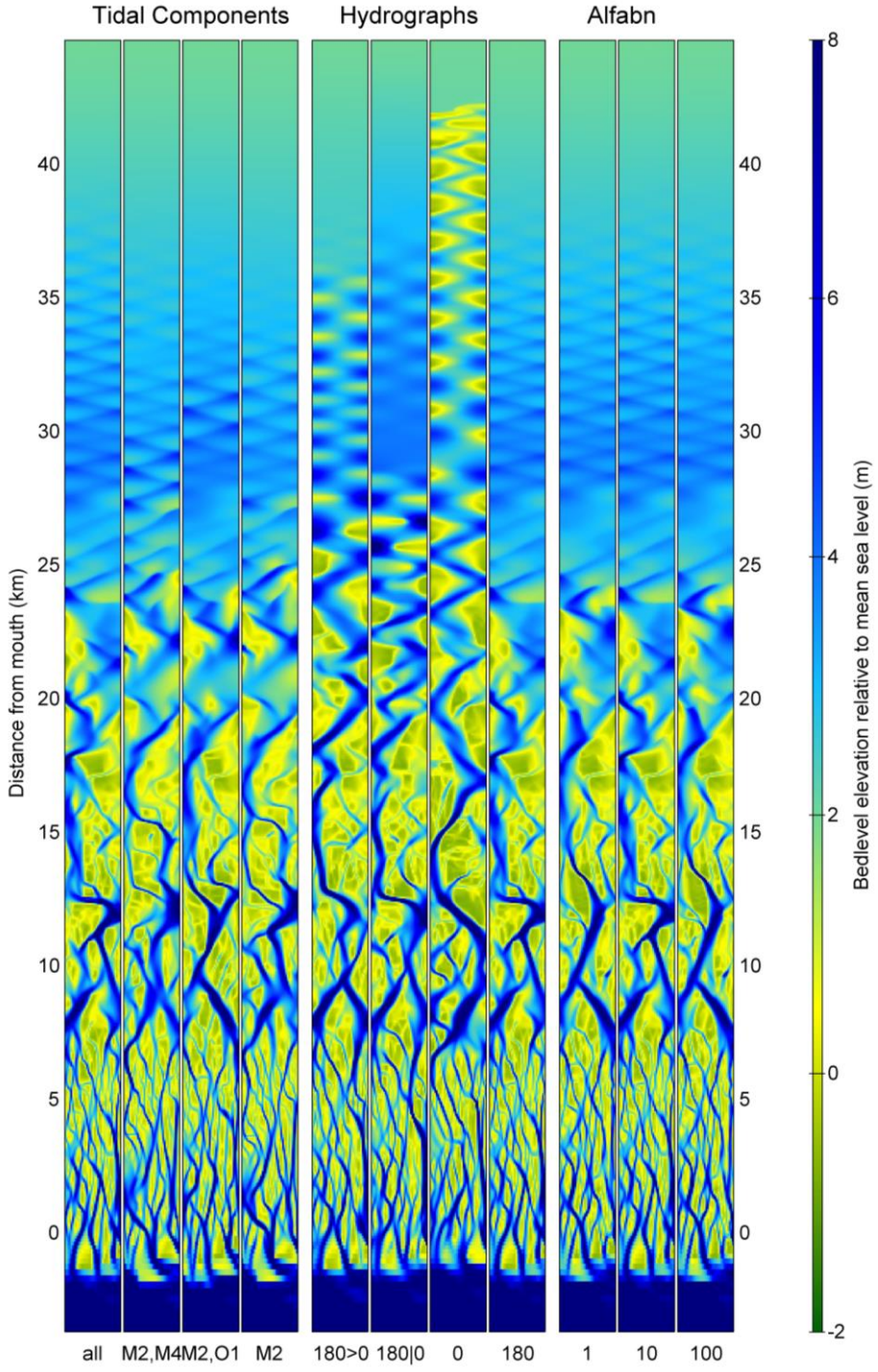

Figure 13: Bed level elevation for distance from estuary mouth against cells that contain the estuary for model runs that vary in tidal components (left), river discharge regime (center) and alfabn (right)..

Shape effect on bed level elevation patterns

The second five subfigures of Figure 12, scenarios which ran the straightened estuary shape, have similar trends compared to the first five figures. Bed level elevation increases with increased river discharge too, in particular in the two highest river discharges. Moreover a similar braiding system exist in the first 5-7 kilometers of the estuary, although less pronounced at the highest river discharge of the straightened scenario. The straightened scenario, similar to the Oer-IJ scenario, without river discharge generates an alternating bar system this bar system develops in a regular system at roughly 20 kilometer from the mouth with a decreasing wave length in landward direction. In contrast to the Oer-IJ scenario the central part of the estuary has always two larger channels coexisting next to each other with mid channel bars in between. This effect does not exist in scenarios with river discharge, those straightened scenarios all have a main channel from 10 kilometer landward, although 180 m^3/s scenario is close to two coexisting channels at 15-20 kilometer. Like the Oer-IJ scenarios, channel bends in straightened scenarios are more elongate with higher river discharge and sharper with lower river discharges.

The idealized trumpet scenarios are the last five subfigures of Figure 12. These scenarios show similar results as the straightened scenarios, in particular regarding bed level elevation. However a few distinct characteristics exist. The braided pattern exist in the idealized trumpet scenario, although the pattern is far more symmetric compared to the straightened and Oer-IJ scenarios. This pattern also extends further landward and a single dominant channel is not reached before 15 kilometer in river discharge scenarios to even 20 kilometer in the no river discharge scenario. Furthermore the high river discharge trumpet scenario has bars that extends farther in seaward direction compared to all previous scenarios.

Effect of other variables on bed level elevation patterns

Figure 13 gives an overview of all model runs that used the reference model (Oer-IJ shape/180 m^3/s) and choose one variable to change.

The first subfigures of Figure 13 show variation in the used tidal components. These variations are relative small, in particular compared to the effect of either river discharge or estuary shape. The lack of the O1 component in both the second and the fourth subfigure looks dominant for the position of the channel within the estuary. These two scenario have similar channel and elevation patterns as well. Moreover increased bed elevations in these scenarios extend further landward as well further seaward. In contrast the third figure without M4 is highest elevated scenario in the central part of the estuary.

In summary elevated bed levels increase further sea and landward the less tidal components are included, though the effect of the removal of O1 is larger than of the removal of M4. Maximum bed level elevations are higher when all tidal components are included. Furthermore most differences exist due difference in the location of channels.

The second subfigure of Figure 13 gives an overview of two different river discharge regimes compared to the high- (180 m^3/s) and low-end (0 m^3/s) constant river discharge regimes. The first subfigure (180>0) shows the linear decrease in river discharge over a hydrodynamic time of one year, this resembles a decrease of 0.45 m^3/s per morphologic year. The second subfigure (180|0) has a constant river discharge of 180 m^3/s for the first six hydrodynamic months, it is thereafter reduced to 0 m^3/s in one month before it remains constant thereafter. This leads roughly to decrease of roughly 5.3 m^3/s per year over a period of 34 years.

The two different discharge regimes are more comparable to each other than to the no and reference river discharge scenarios. In particular in the outer estuary both resemble the reference river discharge scenario. The no river discharge scenario is different to the other scenarios, it extend further and has a slightly different bar pattern. In the central part of the estuary the sudden scenario compares better to the reference scenario than the linear decreased scenario compares to the reference scenario. Hence the effect of the discharge in the first part of the scenario is very important to set up morphology and morphology is only slightly altered in the second half of model run time. This is consistent with the relative equilibrium in the second half of model run time as discussed earlier (Figure 11).

The alfabn parameter variations are minor, the three scenarios are similar to each other, both in pattern and bed level elevation. The reference scenario (alfabn = 10) differentiates more than the other two scenarios, primary as the two other scenarios seem to be copies of each other with barely differences. Overall these differences are not comparable with the changes due difference discharge and shape.

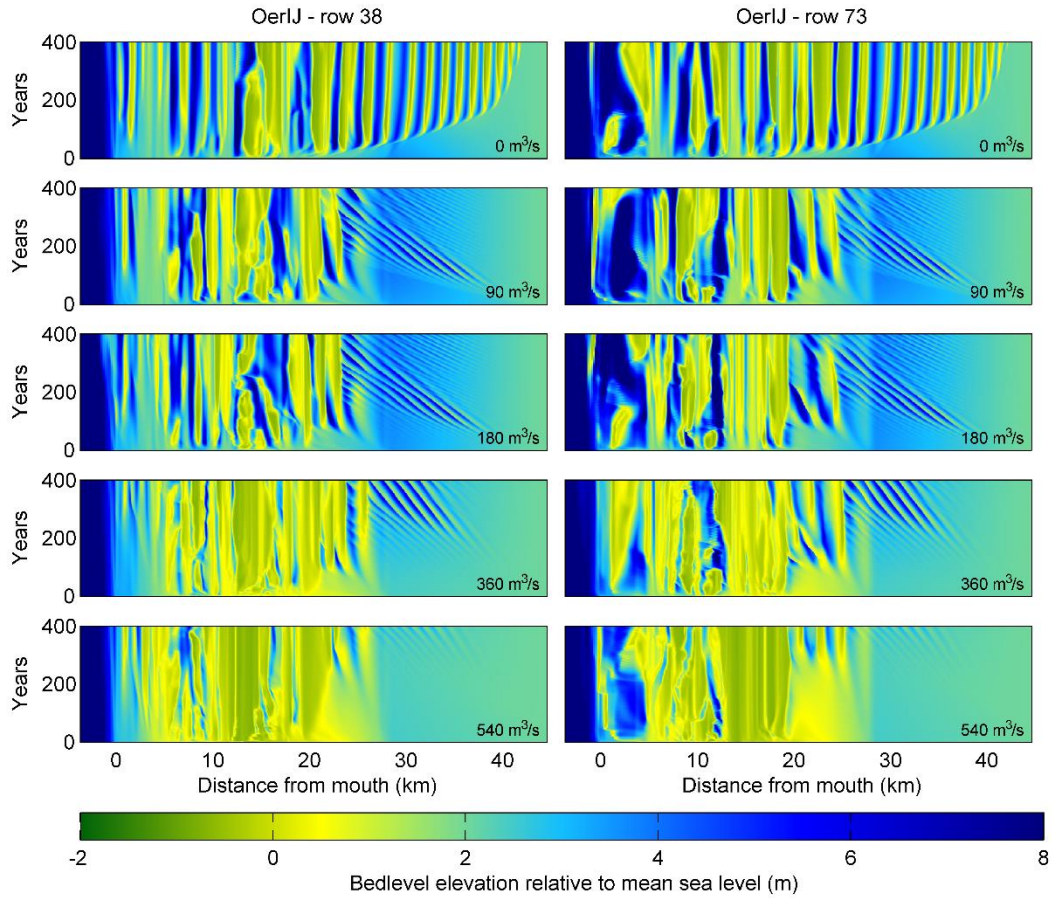

Figure 14: Time space diagram of bed level elevation for the two outlying cells (row 38 is northern, row 73 is southern) for five different river discharges of the Oer-IJ shaped scenarios.

Bar migration at the boundaries of the estuary

Dynamics of the estuary can also be presented by the mobility of bars, whether these bars migrate landward or seaward or whether these bars do not migrate at all. The time-space diagrams of Figure 14, Figure 15 and Figure 16 presents the behavior of bars at the side of the estuary. In these figures bed elevation is shown as a function of distance from the estuary mouth over time. The most northern (lowest row number) and southern (highest row number) located row of grid cells are chosen to see in particular the effect of dynamic bars in the upper and river part of the estuary. The subfigures indicate different river discharge input.

Overall these figures display two type of bars within the estuary, migrating and fixed bars. The migrating bars are primary found over 25 kilometer from the mouth but do not exist in the no discharge scenarios. The fixed bars are most often formed in the first 100 year and are found in both the central and outer parts of the estuary in all scenarios, although they are more pronounced at both lower discharges and less complex shapes.

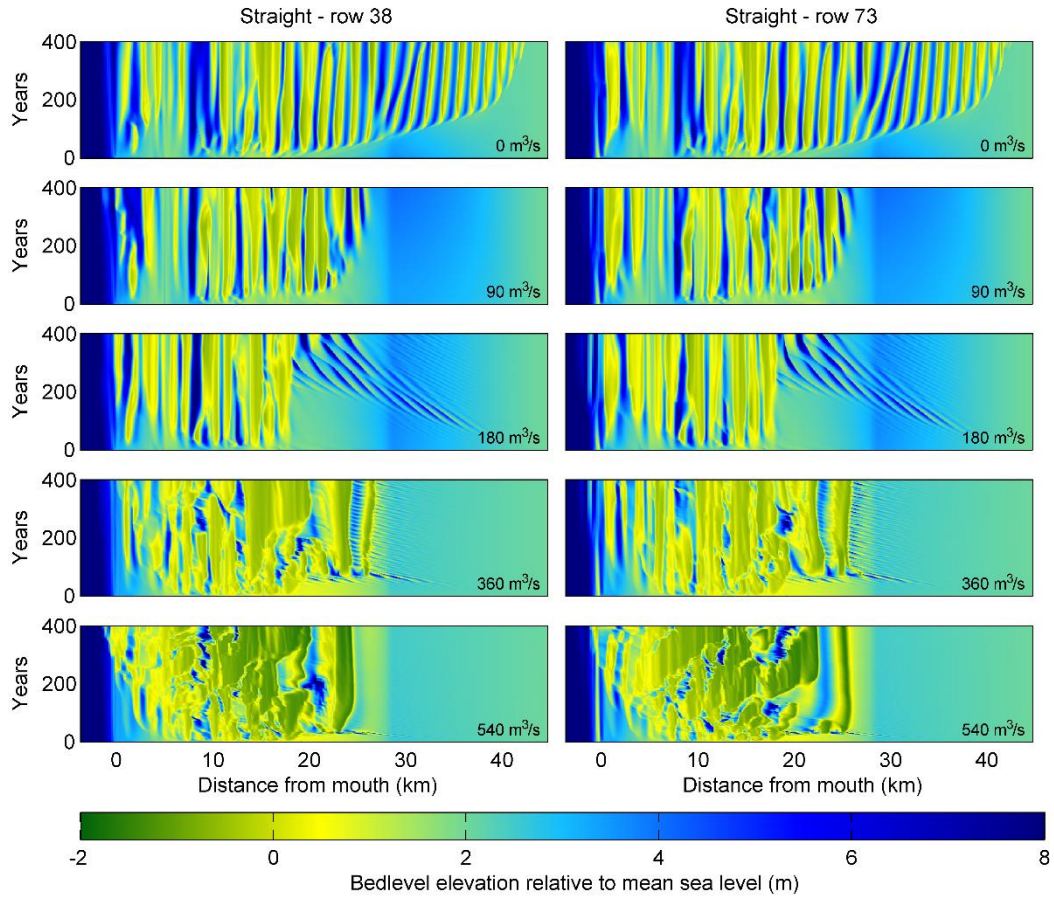

Figure 15: Time space diagram of bed level elevation for the two outlying cells (row 38 is northern, row 73 is southern) for five different river discharges of the straightened shaped scenarios.

Effect of river discharge on bar migration

The Oer-IJ scenarios (Figure 14) are very dependent on river discharge. The no river discharge scenario (upper figures) is dominated by far inland progressing alternating bars. This scenario shows almost time independent bars on both sides of the scenario. These bars move slightly landward after initial formation but remain fixed soon thereafter. Bars are formed first in the central part of the estuary and are formed further landward thereafter. In landward direction the bars are positioned closer to each other and the bar length slightly increases too. In the outer and central part of the estuary no such rhythm exist, channels behaves more dynamic as explained by the irregular shapes. Bars in the outer part of the estuary nevertheless remain fixed once formed, channel migration is able to destroy a bar once formed but the bars do not migrate through the outer part of the estuary.

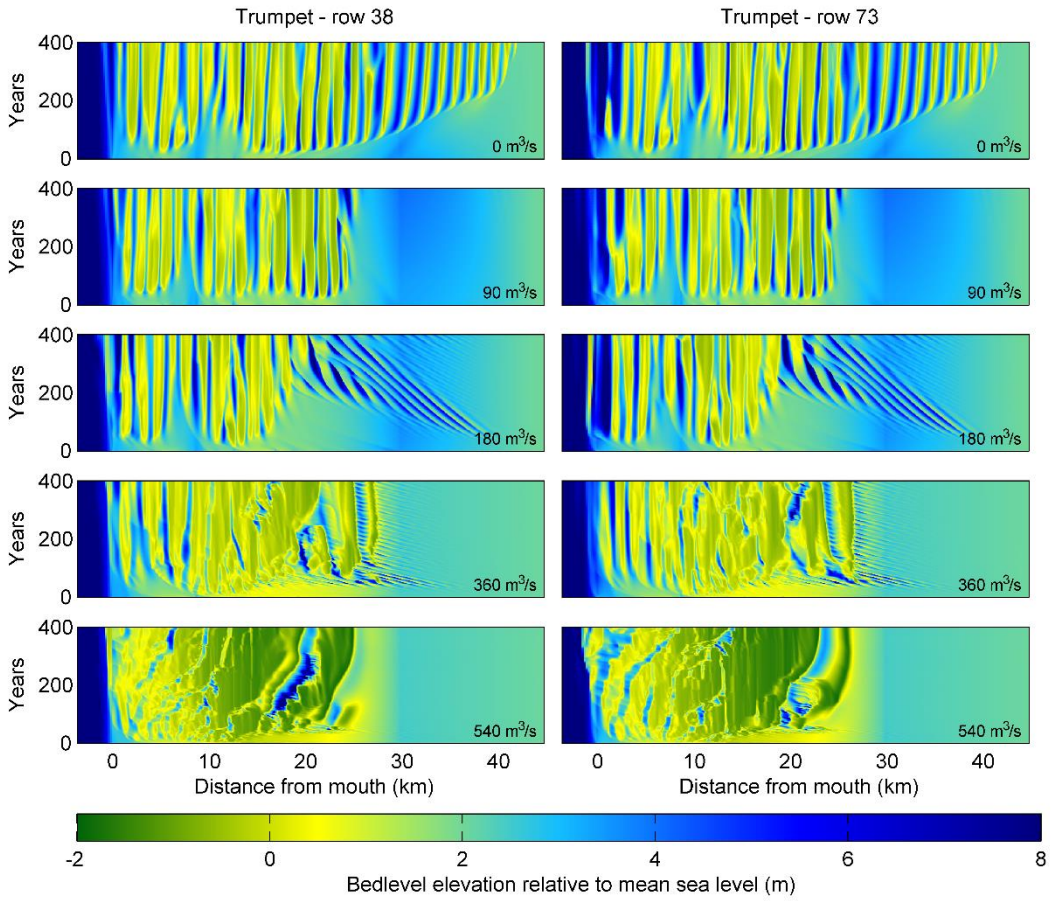

Figure 16: Time space diagram of bed level elevation for the two outlying cells (row 38 is northern, row 73 is southern) for five different river discharges of the idealized trumpet shaped scenarios.

The introduction of river discharge results in a slightly different behavior, the bars at the inner part of the estuary are not fixed and with even increased discharge bars in the central estuary become longer and more elevated. The bars in the inner estuary all migrate in seaward direction, nevertheless migration speed both within one scenario over time or over distance and between the scenarios is not fixed. In all scenarios the most landward positioned fixed bar is around 25 kilometer from the mouth. This bar is more pronounced with higher discharges and is positioned slightly more inland but it exist in all scenarios.

Effect of estuary shape on bar migration

The straightened scenarios (Figure 15) behave similar as the Oer-IJ scenario, there are several differences nonetheless. In the no river discharge straightened scenario the bars in the central part are fixed like the Oer-IJ scenario. The inner estuarine alternating bars move slightly landward after formation as well. A more dynamic behavior exist between the fixed and migrating bars. At least one new bar is here formed in the second half of the model run. Alternating migrating bars do exist at the scenarios with river discharge in the upper part of the estuary, though are only very pronounced in the middle river discharge scenario (180 m^3/s). This scenario differs quite some as the last fixed bars are both located further seaward (only 20 kilometer from the mouth) and are relative young (formed after 300 years).
The idealized trumpet scenarios (Figure 16) are very stable. Almost all bars are fixed and formed relative fast. A slight delay exist just before 10 kilometer from the mouth, a location where the initial bathymetry was less shallow. Like the straightened scenario, the middle river discharge scenario for the idealized trumpet shape is the only idealized trumpet scenario with pronounced migrating alternating bars in the upper estuary. The highest river discharge idealized trumpet scenario gives a clear channel migration in landward direction over the entire estuary although the pace of migration is slowed when time progresses.

Overall these figures indicate that these scenarios are relative stable, most variation is seen in the first 150 years, thereafter variation is minor or constant. This is consistent with the previous parts in which the estuarine patterns remained stable in the second part of the modelling time.

Flow velocity

Apart from bed level elevation, flow direction and flow velocity are just as important to explain the behavior of certain features. Quite a number of features can be either flood or ebb dominant. Residual flow velocities are displayed in Figure 17 for three different shapes and river discharges. Residual flow velocity is computed by taking the mean flow velocity over one M2 period for each cell. This residual flow velocity gives an overview at what location water is predominant flowing in seaward direction (negative) or in landward direction (positive). The residual flow patterns are very similar to the bed level elevations of Figure 12, nevertheless some interesting characteristics can be noticed.

The no river discharge scenario shows that water flows predominantly seaward in the channel and predominant landward on the bars, in particular close to the channel. An effect that corresponds with other studies (Brown & Davies 2010). This effect is less pronounced in the outer part of the estuary. Moreover with an increased river discharge the residual flow velocity in the channels increases and the residual flow velocity over the banks is reduced. With maximum river discharge the residual flow is directed in seaward direction only, nevertheless channels still have a significant higher residual flow velocity.

Straightened and idealized trumpet scenarios show the similar characteristics, although the higher river discharge scenarios show residual flow velocities that are even higher compared to the Oer-IJ shape with similar river discharges. This feature may indicate a shallower depth in the straightened and idealized trumpet scenarios, an effect which will be discussed later. Moreover the residual flow velocity in in particular the middle river discharge scenarios distinguishes relative well between main and secondary channels, where the main channel has higher residual flow velocities.

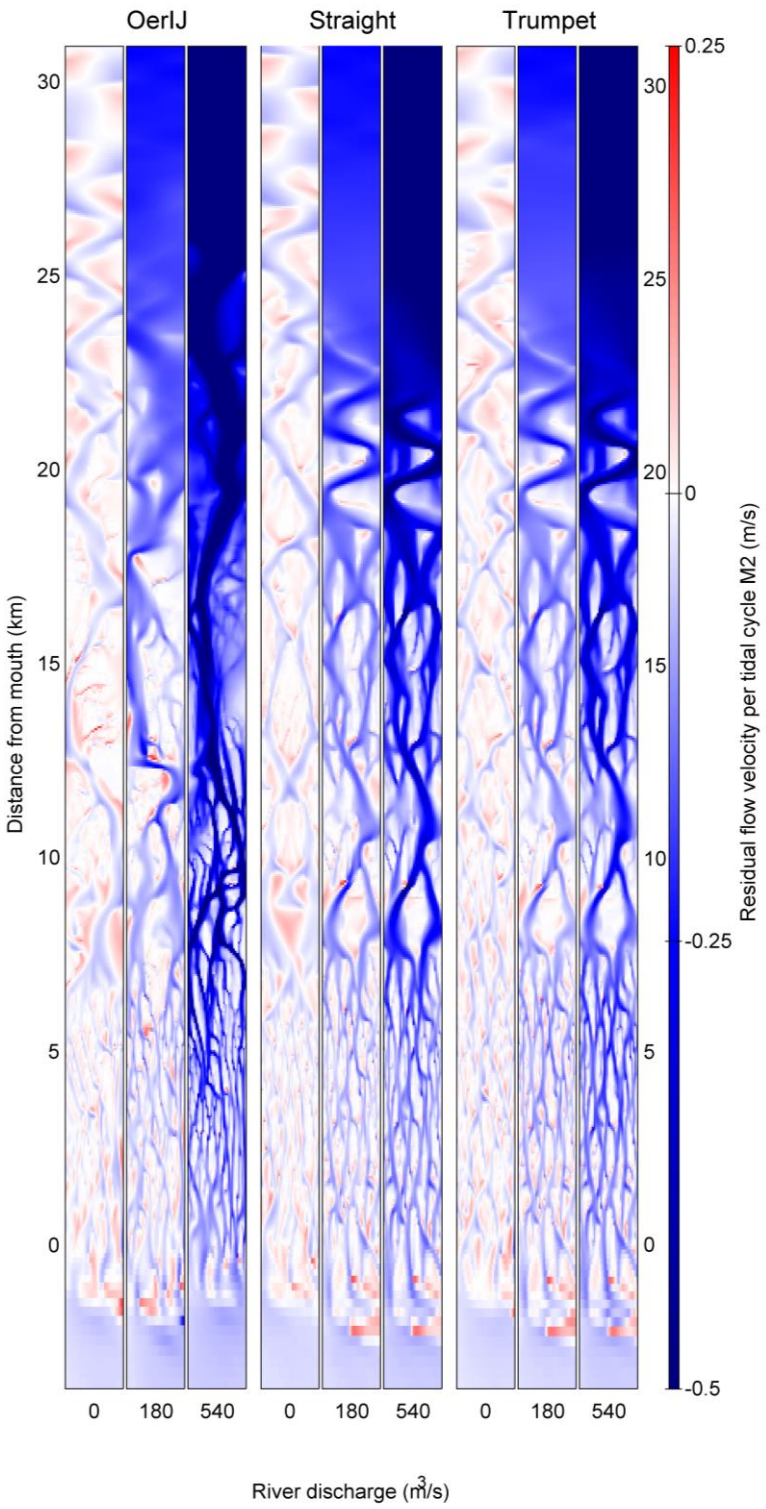

Figure 17: Residual flow velocity for no, medium and high river discharge for Oer-IJ, straightened and idealized trumpet scenarios for each cell in the estuary.

Width averaged representation of the model results

In the above section the results were all represented in a map view. A more quantitative overview of several parameters can be done in a width averaged representation. In this representation different parameters are presented as an average or maximum over the width of the estuary. Figure 18, Figure 19 and Figure 20 give this representation for the three different shape scenarios. The columns represent the no river discharge, medium river discharge (180 m^3/s) and high river discharge (540 m^3/s) scenarios. The first row shows both bed level and water level, where bed level values are taken from the last map file of bed level elevation and water level is taken over a window of six times M2 period per grid cell. The second row is the braiding index, the number of parallel channels per unit width (Marra et al. 2014). This braiding index is determined from the final bed level elevation that is compared with minimum and maximum water levels as displayed in the first row. Any bed level elevation between high and low water is assigned as a 'bar' cell, any bed level elevation below low water is assigned as 'channel' cell. Every shift from channel to bar in neighboring cells over estuary width increases braiding index with 1. The third row represents the percentage of intertidal area, a percentage where is accounted for the area of each of the cells in a cross-section. The final row represents three equal figures of the width of the estuary, these sub-figures will differ in different shape scenarios and are similar to Figure 8.

Effect of river discharge on width averaged parameters

The first row of Figure 18 show a very distinct effect of river discharge, both on water level and bed level elevation. Water level in the estuary remains constant over distance without any river discharge, both the low and high water level increase slightly with an increased river discharge. This effect is minor compared to the maximum river discharge scenario. At this scenario the high water level increases significant more over the length of the estuary. Moreover the low water level suddenly raises very fast over the length of the estuary. In roughly 5 kilometer low water level increases from similar value as the previous scenarios to a value just below the high water level. Thereby it reduces the difference between high and low water to even less than a quarter of its former difference.

Bed level elevation marks another trend, apart from the numerous peaks it is clearly visible that both the low and mean bed level are more elevated in the high river discharge scenario compared to the other two scenarios. The difference between the no and middle river discharge scenarios is smaller but the no river discharge scenario is still somewhat lower than the middle river discharge scenario. Moreover mean bed level elevation in the central part of the model (between 10 and 20 kilometer) is the most elevated part of the model. This is only overtopped by the most upstream part in the no river discharge scenario, where relative large alternating bars were formed, which raises in particular mean and max bed level elevation. These bars are less pronounced in other scenarios but exist in all.

The percentage of intertidal area (third row) indicates another trend. Intertidal areas do not extend far landward in the high discharge scenario, after 15 kilometer intertidal area is reduced to a minimum. This length is increased for the middle discharge to 20-25 kilometer and even further increased with no river discharge to almost 30 kilometer (when the upstream peaks that are generated by alternating bars are neglected). Next to a decrease in length of intertidal area with increased river discharge, the percentage of intertidal area per unit width is of similar order in all scenarios. Nevertheless the highest river discharge scenario shows the highest percentage of intertidal area in the outer part, up to 10 kilometer from the mouth, while the other two scenarios show the highest percentage of intertidal area in the inner part (10-

20 kilometer). In all scenarios these two parts are divided by small part without intertidal area located just within 10 kilometers of the mouth which coincides with the most seaward narrow passage in the estuary.

This division of two parts of the estuary can be recognized in braiding index (second row) too. The braiding index is higher in the first 10 kilometers compared to the second 10 kilometers in all scenarios. However where in the high river discharge scenario high braiding index correlate with a large percentage of intertidal area, in the lower river discharge scenarios high braiding index correlates with a smaller percentage of intertidal area on the contrary. As such no relation between percentage of intertidal area and braiding index can be distinguished. Finally all scenarios present the single channel that exist after 20 kilometers that correlates with the map results.

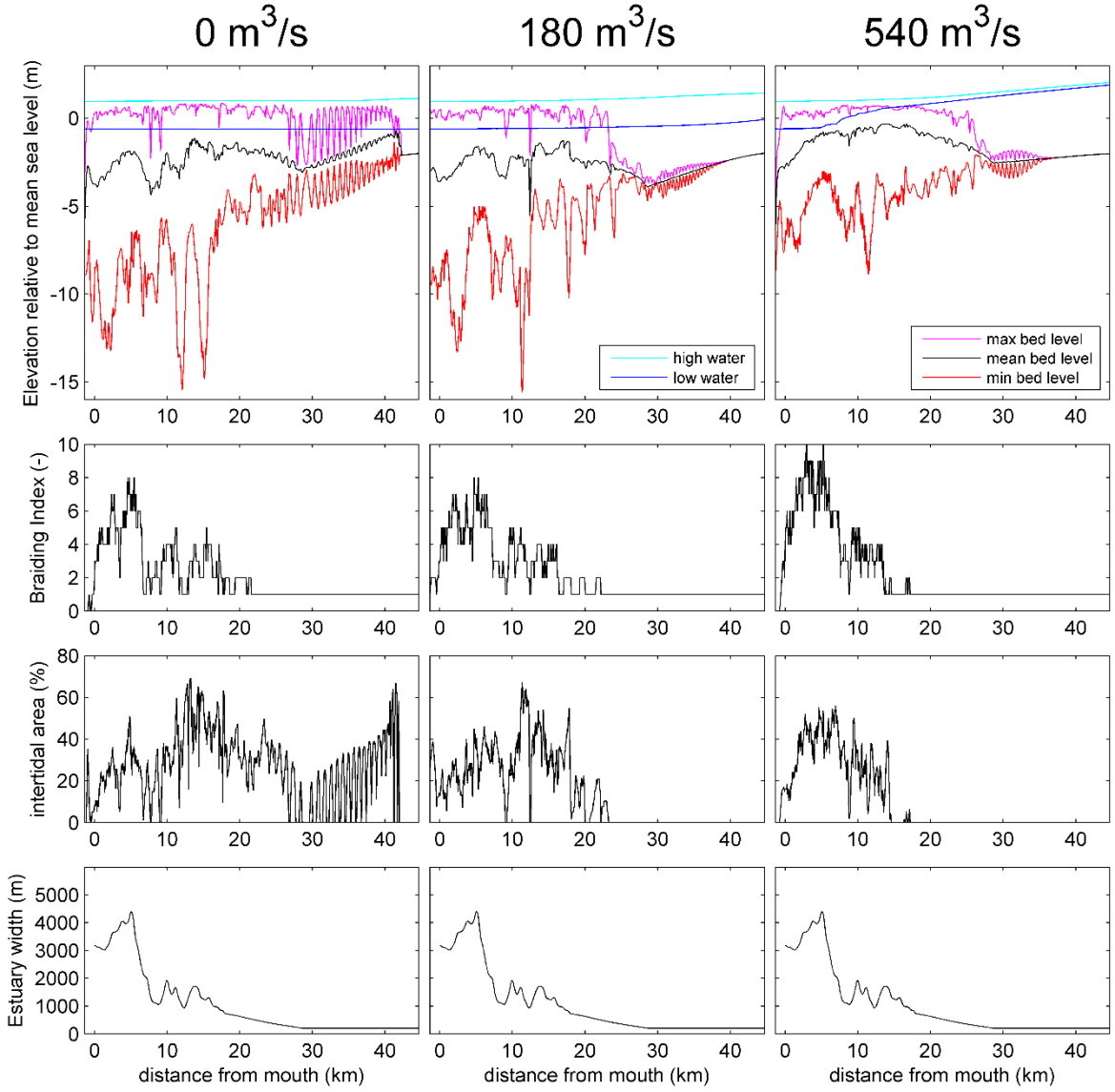

Figure 18: Longitudinal profiles of bed and water level elevation, braiding index, percentage of intertidal area and estuary width for no, medium and high river discharge Oer-IJ shape scenarios.

Effect of shape on width averaged parameters

The straightened scenarios (Figure 19) have both similarities and differences with the Oer-IJ scenarios (Figure 18). The major difference regarding water level is that the no and middle river discharge scenarios behave like the Oer-IJ scenario but the high river discharge scenario lack the sudden increase in low water level which was characteristic for the high river discharge scenario in the Oer-IJ, the water level increases nonetheless though with more gentle increase and with less reduction of tidal range.

Bed level elevation increases significant in the high river discharge scenario, in particular the mean bed level and the maximum bed level. The latter even overtops high water levels, which may indicate higher water in an earlier part of the model. On the contrary bed level elevation in the straightened and Oer-IJ scenarios are very similar in lower discharge scenarios.

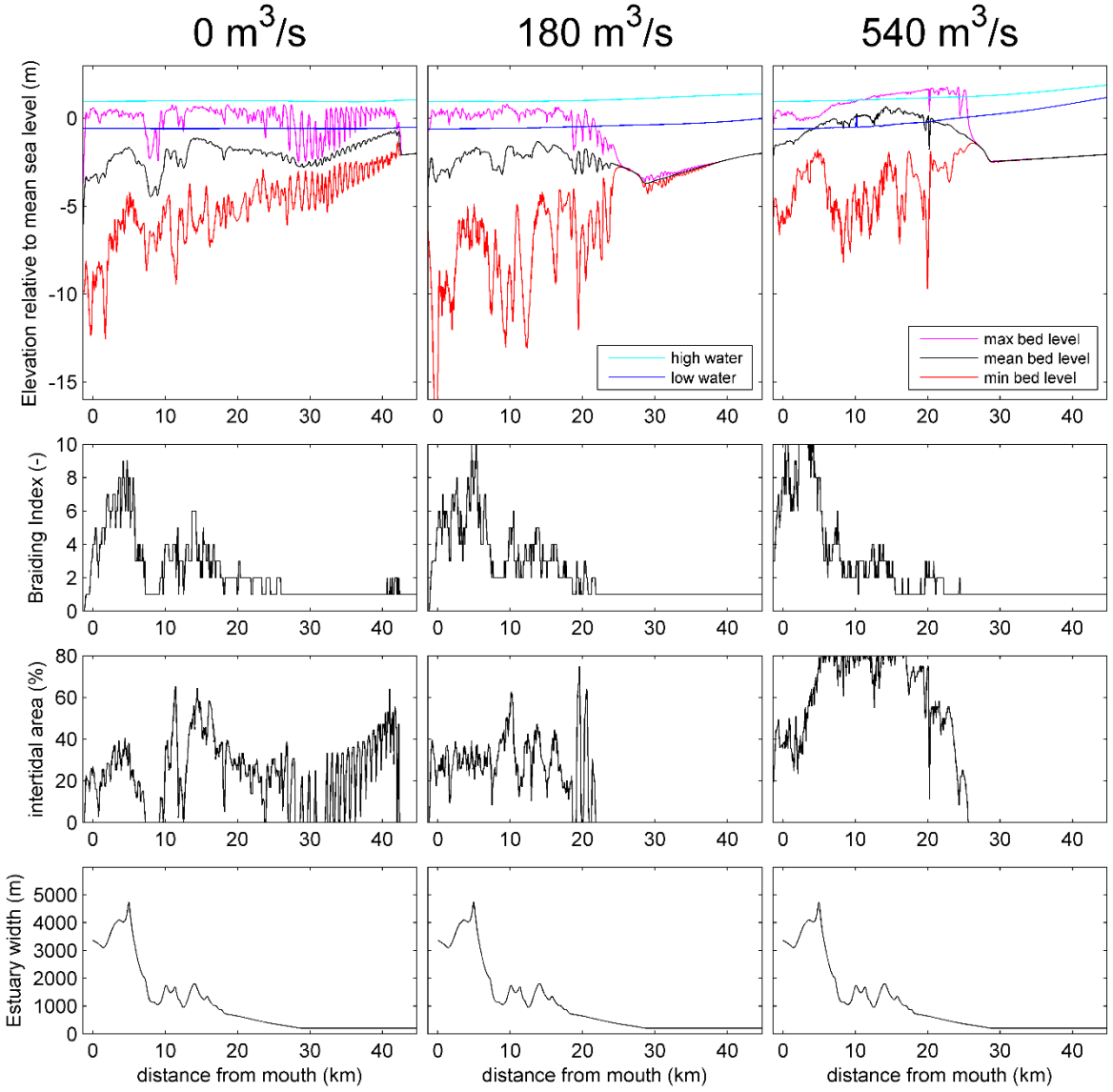

Figure 19: Longitudinal profiles of bed and water level elevation, braiding index, percentage of intertidal area and estuary width for no, medium and high river discharge for straightened shape scenarios.

Braiding index shows a similar pattern, like the Oer-IJ scenarios there is a split in the estuary just before 10 kilometer where the first part of the estuary has a larger braiding index. In contrast to the Oer-IJ scenarios, the straightened scenarios keep multiple channels further from the estuary mouth. All Oer-IJ scenarios reached a single channel state before 20 kilometer whereas all straightened scenarios reach a single channel state far over 20 kilometer up to even 25 kilometer.

The percentage of intertidal area in the no river discharge and middle river discharge scenarios is similar to the coinciding Oer-IJ scenarios, both in magnitude and difference between the first and second part of the estuary. Although the difference in intertidal area between outer and inner estuary has been flatted in the middle river discharge scenario. This percentage of intertidal area increases drastically in the high river discharge scenario, up to 80-90 percent is reached between 5 and 20 kilometer. Moreover intertidal area exist here up to 25 kilometer in contrast to up to 15 kilometer in the Oer-IJ scenario. A behavior that is possibly caused by a bed level higher than the high water level.

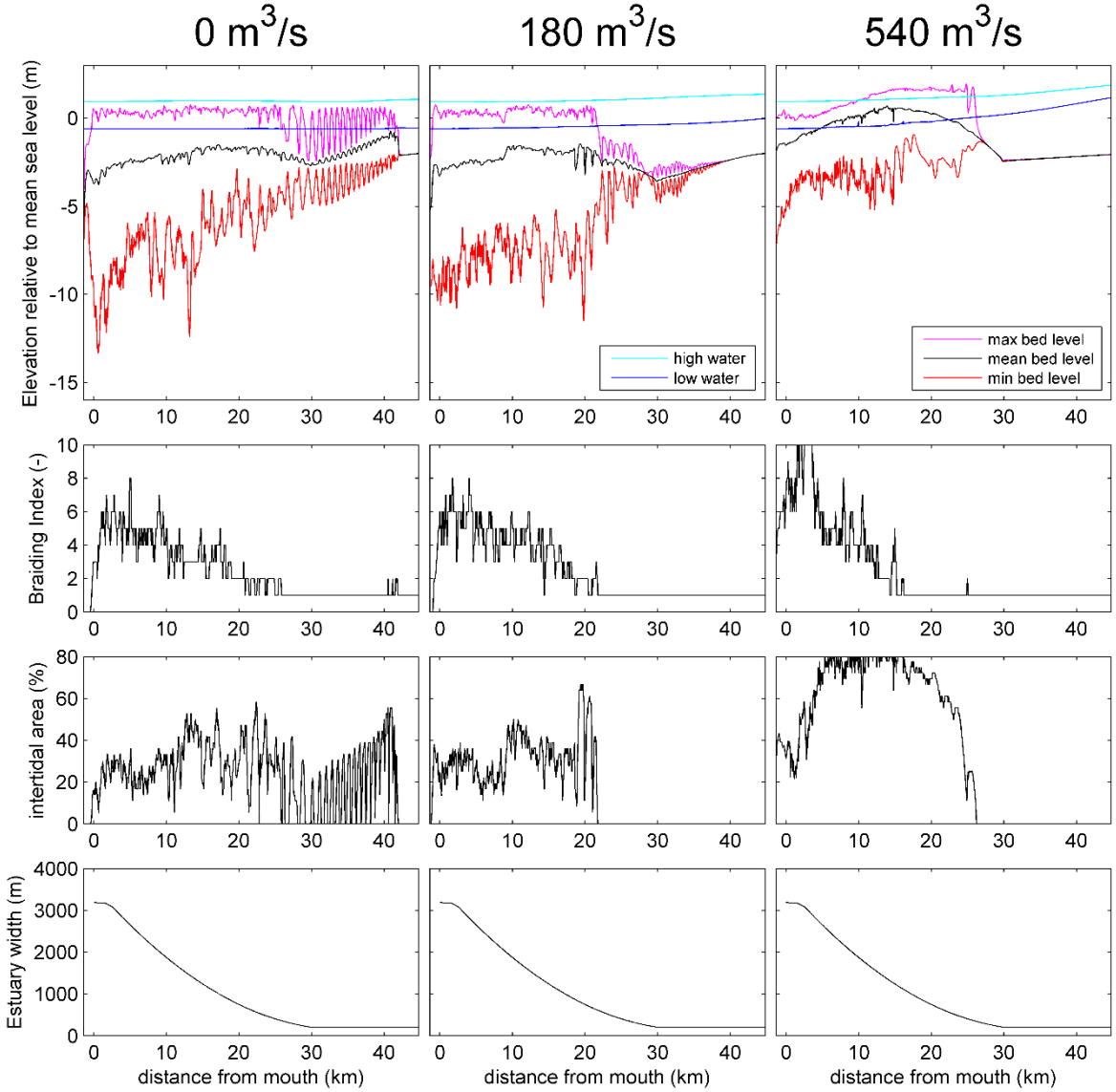

Figure 20: Longitudinal profiles of bed and water level elevation, braiding index, percentage of intertidal area and estuary width for no, medium and high river discharge for idealized trumpet shape scenarios.

The idealized trumpet scenarios (Figure 20) differ slightly from the other scenarios, the width in these scenario is reduced at a regular pace, thereby removing bottlenecks in the previous scenarios that often coincided with characteristic breakpoints.
High and low water levels are similar to the water levels in the straightened scenarios. Bed level elevation is also very similar to the straightened scenarios, however both the mean and minimum bed level elevation are more smoothed in comparison to the straightened scenarios.
Braiding index on the contrary shows a clear distinction to previous scenarios. All scenarios show a decreasing braiding index in landward direction, whereas the previous scenarios had not such clear relation. Moreover braiding depends on river discharge, an increased river discharge generates a higher maximum braiding index. However with an increased river discharge the braiding index is reduced to one channel over much shorter distances, 15 kilometer for high river discharge in comparison to over 25 kilometer in no river discharge scenarios, the middle river discharge scenario is positioned in between with just over 20 kilometer before a single channel is reached.
The percentage of intertidal area is not related with braiding index. On the contrary the percentage of intertidal area is very similar to the straight scenario, just a bit more smoothed like bed level elevation in the first row of subfigures.

Overall the shape effect are most dominant in the high river discharge scenarios. In both the idealized trumpet and straightened high river discharge scenario the bed level elevation is higher compared to the Oer-IJ scenario, in particular the maximum and mean bed level elevation. Likewise the low water level is significant lower in these scenarios compared to the Oer-IJ high river discharge scenario, which thereby results in a higher tidal range. The high river discharge scenarios for straightened and idealized trumpet shapes show also a higher percentage of intertidal area. Upon comparing both the idealized trumpet scenarios and the straightened scenarios there is one small difference, idealized trumpet scenarios show smoother bed levels, braiding index and percentage of intertidal area compared to the latter.

Bed level elevation over time.

Figure 11 shows map results over time, Figure 21, Figure 22 and Figure 23 show the mean bed level elevation over time. The irregular initial profiles (red lines in further time steps) are overall very dominant as main elevation differences come primarily from these initial profiles, change is limited in further time steps.
Figure 21 visualizes the differences between three different river discharge regimes, the scenarios are similar to the scenarios in the map view over time (Figure 11). In all scenarios there exist a slight decrease in bed level elevation over time, this sediment is transported mostly in seaward direction as estuary slowly extends further seaward in all scenarios.
Figure 22 compares different river discharge scenarios, hence it is clearly visible the high river discharge scenario has a far higher bed level elevation. In this scenario it is remarkable that the bed level decreases in the inner estuary and increases in the outer estuary, an effect unique in this scenario. The bed level elevation in the no river discharge scenario has an opposite behavior, here bed level elevation decreases in the outer estuary and increases in the inner estuary. The middle river discharge scenario has a no clear trend. Figure 23 compares different shapes, these graphs are relative similar, most notable is that the Oer-IJ and straightened scenarios keep the initial irregular profile while the idealized trumpet scenario tends to smoothen this initial profile over time.

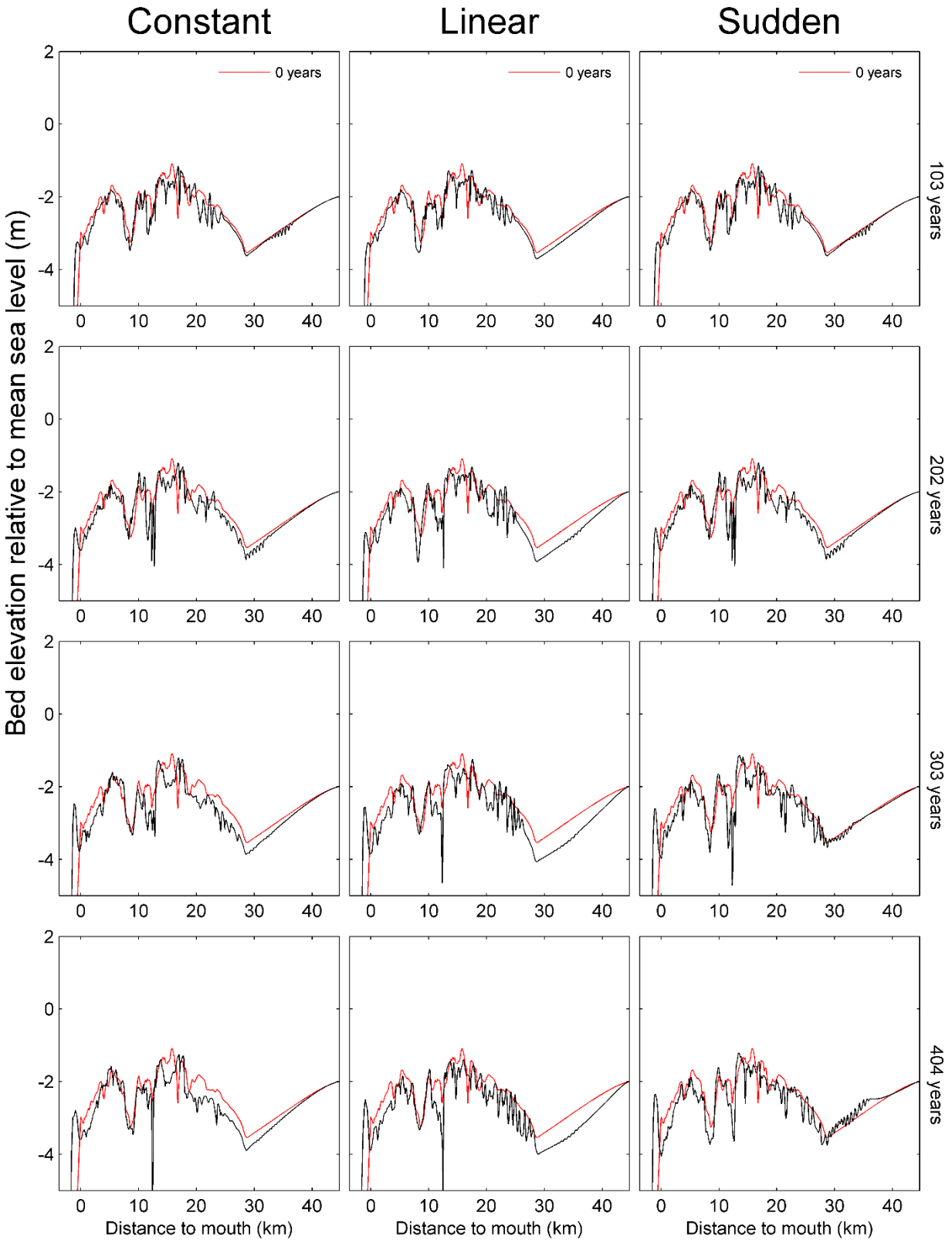

Figure 21: Mean bed level elevation over time as function of distance from mouth for constant, linear decreasing or sudden decreasing river discharge for the Oer-IJ scenario.

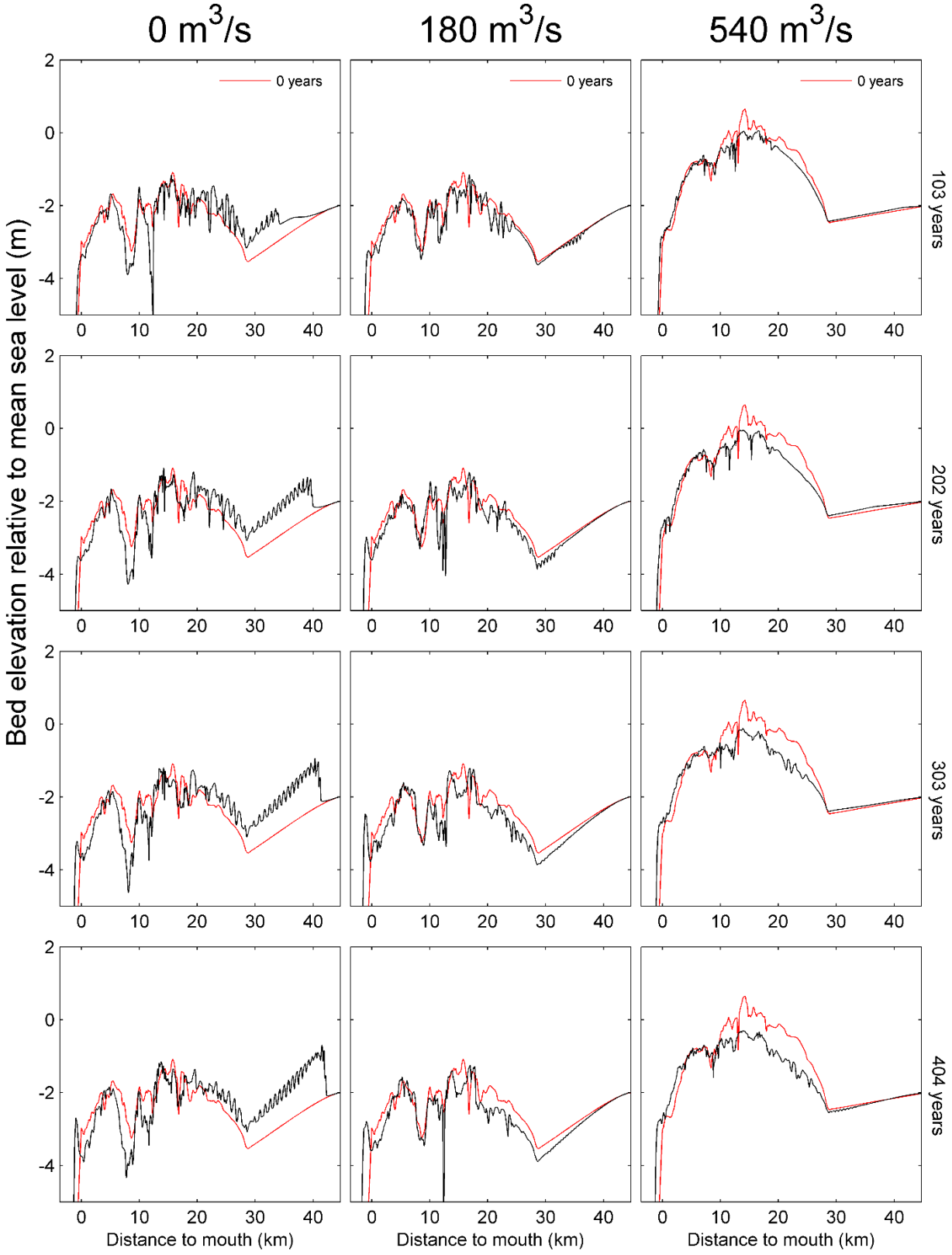

Figure 22: Mean bed level elevation over time as function of distance from the mouth for no, medium and high river discharge Oer-IJ scenarios.

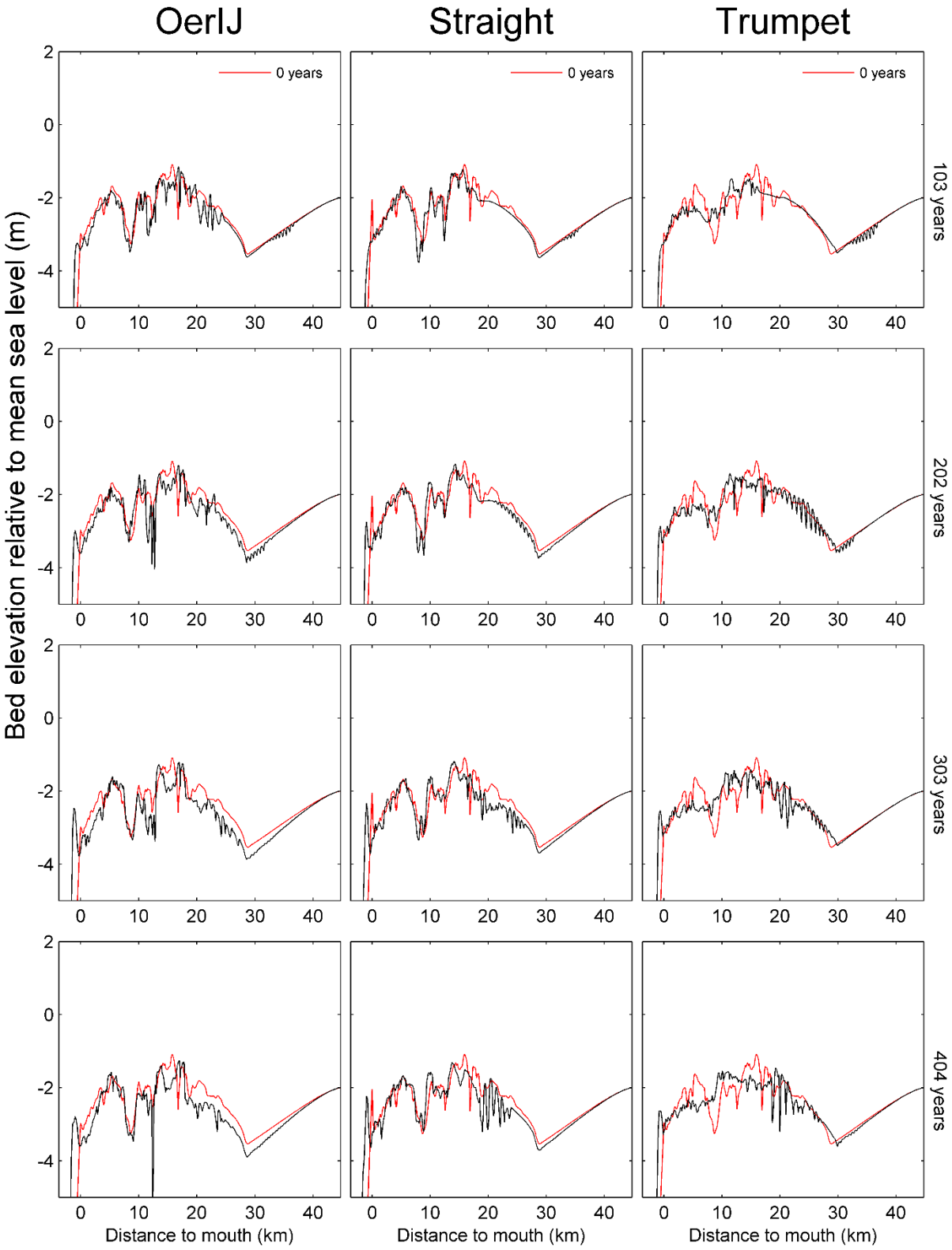

Figure 23: Mean bed level elevation over time as function of distance from the mouth for Oer-IJ, straightened and idealized trumpet middle river discharge scenarios.

Numerical Comparison

Figure 24 gives an overview of the effect of different variables in our model runs. The first column is the effect of river discharge plotted against important tidal parameters. In this first column the comparison between different shapes is shown in color. The second column summarize the effect of the alfabn variable while the third column summarizes the effect of different components of the tidal signal used at the seaward boundary.

Mean absolute discharge (first row Figure 24) is an indication of the amount of water which enters and exit an estuary through the estuary mouth:

$$\bar{Q} = \frac{1}{T}\int_0^T |Q_m|\, dt - Q_r$$

wherein T is the period of M2 in seconds, Q_m is the total water flow through the mouth of the estuary over time (m^3/s), Q_r is the river discharge (m^3/s) at the river boundary and $\bar{Q}$ is the mean absolute discharge (m^3/s). Tidal prism can be derived by multiplication with the M2 period and obvious has a similar trend as mean absolute discharge.

Tidal range is taken as the difference between maximum water level and minimum water level from the hydrodynamic runs. The values presented in Figure 24 are taken at a distance of 10 kilometers from the estuary mouth. Closer to the mouth the tidal range varies less, further landward the tidal range varies more between different scenarios, nevertheless the trend is similar in all locations.

The cross-sectional area is a variable which is often used in combination with tidal prism:

$$A = CPn$$

wherein A is the characteristic cross-sectional area (m^2), P is the tidal prism (m^3), C is a constant with unit depending on n and n is a coefficient (-)(Van der Wegen et al. 2010). The third row of Figure 24 gives an overview of cross-sectional area, this area is taken cell wise from mean water elevation at the mouth minus the bed level elevation at the mouth and multiplied by the width of each individual cell.

Braiding index (BI) is an indication of river pattern and is determined by the number of parallel channels in the confinement. Braiding index was elaborated in Figure 18, Figure 19 and Figure 20 and two different parts of the estuary were determined in that section, the inner and outer estuary. Figure 24shows braiding index in both the inner and outer estuary, the boundary is taken between grid cell 200 and 201 located at 8.5 km from the estuary mouth, the upper boundary of the inner estuary is taken at cell 350 at 16 km from the mouth.

Intertidal area is an indication what part of the total estuary area becomes dry at low water and is flooded at high water. The percentage used in the fourth row of Figure 24 is as such computed. Intertidal area is calculated as the sum of every cell with a bed level elevation above minimum water level elevation of a row of cells. The fraction of intertidal area is thereafter computed with the total area of the estuary. The split up in an inner and outer part as seen in Figure 24 and mentioned above under braiding index is similar to the definition of inner and outer estuary in the braiding index section.
Mean bed level elevation is defined as the mean of the final bed level elevation for respective the inner and outer estuary. As a result both channels and bars are part of the mean bed level elevation.

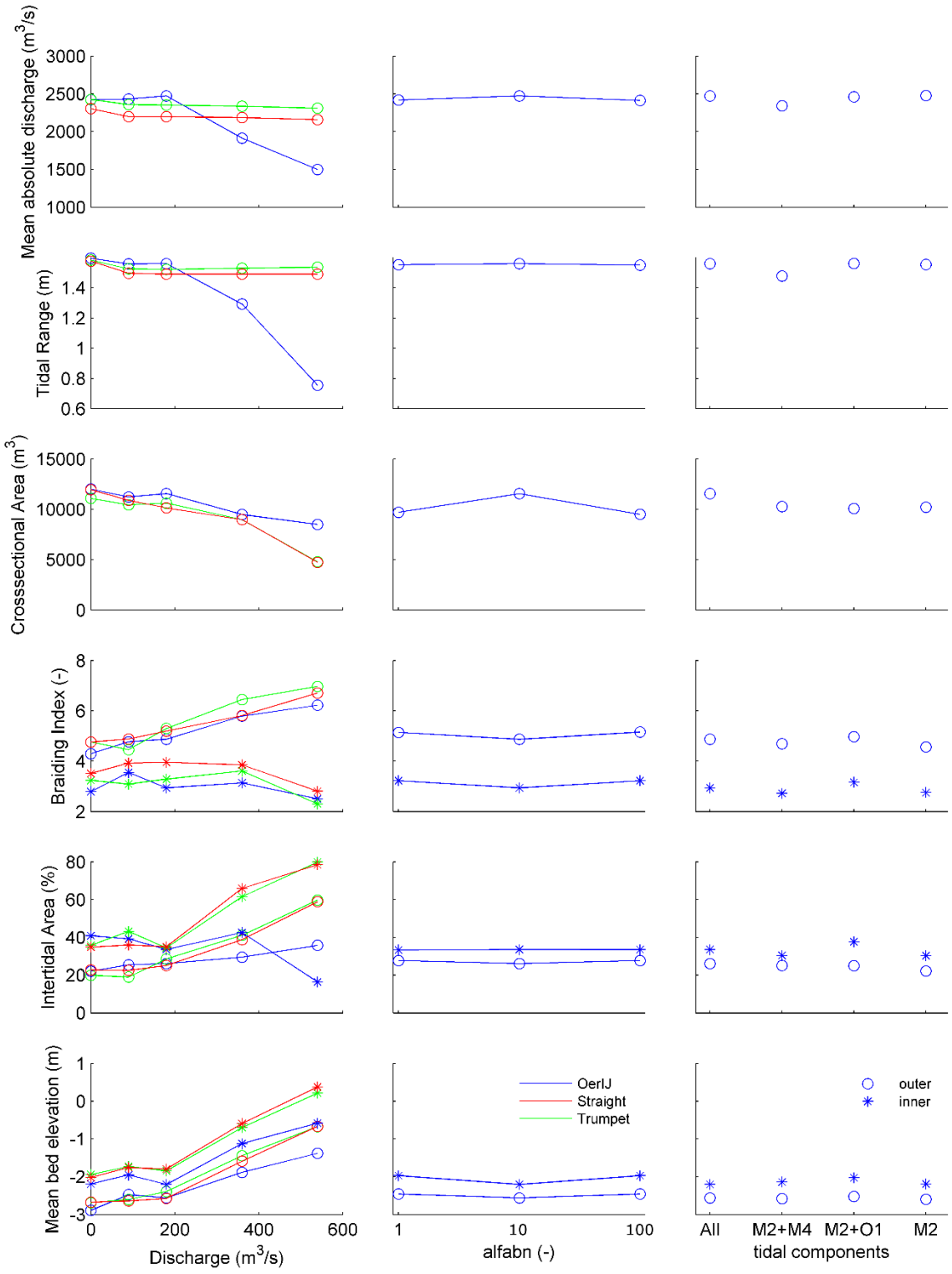

Figure 24: Numerical overview of mean absolute discharge at the mouth of the estuary, tidal range at 10 km from the mouth, and cross-sectional area at the mouth. As well braiding index, percentage of intertidal area and mean bed level elevation for both inner (< 10km from the mouth) and outer (> 10km from the mouth) against the used variables river discharge, alfabn and tidal components for Oer-IJ (blue), straightened (red) and idealized trumpet (green) scenarios.

The combined effect of river discharge and estuary shape on numerical parameters

The mean absolute discharge is almost constant as function of river discharge in the straight and idealized trumpet scenarios. Mean absolute discharge is highest without river discharge and decreases slightly with increasing river discharge, river discharges over 100 m^3/s barely effect the mean absolute discharge. The idealized trumpet shaped scenarios have a slightly increased mean absolute discharge compared to the straightened shaped scenarios. This effect is expected to be caused by a slightly smaller opening of the initial grid of the straightened estuary compared to the other two shape scenarios. As the trend in these two scenarios is similar, small differences will not be discussed further. On the contrary the curve of mean absolute discharge over river discharge for the Oer-IJ scenarios is more characteristic. In these scenarios the mean absolute discharge increases slightly up to 200 m^3/s river discharge, the two scenarios with highest river discharge (360 and 540 m^3/s) give a steep decrease in mean absolute discharge with increased river discharge, a roughly linear decrease.

Like mean absolute discharge the tidal range is similar in the straightened and idealized trumpet scenarios, moreover apart from a small decrease in tidal range from no to 90 m^3/s river discharge the tidal range remains relative constant. Likewise tidal range behaves similar to mean absolute discharge in the Oer-IJ scenarios. Tidal range decreases less with increased river discharges up to 200 m^3/s compared to the other scenarios, thereafter tidal range decreases rapidly with increased river discharge, an almost exponential decrease.

Figure 24 shows a negative relation between cross-sectional area and river discharge. In all scenarios increased river discharge causes a decreased cross-sectional area, where cross-sectional area is halved within this range of river discharges. The Oer-IJ scenario differs in this parameter only at the highest discharge, where cross-sectional area is reduced less compared to the other scenarios.

Braiding index variations between the Oer-IJ and other scenarios are relative minor, although BI for the Oer-IJ scenarios is often lowest of all scenarios. Braiding index in the outer estuary increases in all scenarios with increased river discharge, at roughly 1 for every 100 m^3/s. Braiding index in the inner estuary is low at no river discharge, slightly higher with river discharges up to 400 m^3/s but thereafter decreases towards the highest river discharge in our model scenarios. Overall braiding index is significant higher in the outer estuary compared to the inner estuary.

Intertidal area in straightened and idealized trumpet scenarios is roughly similar as seen in Figure 24, the intertidal area in the Oer-IJ scenarios is similar for river discharges up to 200 m^3/s too. A further increase in river discharge causes intertidal area in straight and trumpet scenarios to increase. In contrast the intertidal area in the Oer-IJ scenario only slightly increase and as such results in a significant lower intertidal area for high river discharges. For the highest river discharge scenario the inner estuary intertidal area is even lower than the outer estuary intertidal area. Finally all scenarios of 180 m^3/s are very similar to each other, despite different confined shapes and differentiation between inner or outer estuary.

The final row of Figure 24 shows a clear relation between bed level elevation and river discharge. In all scenarios an increased river discharge increases bed level elevation in both inner and outer estuary. Bed level elevation in the inner estuary is always higher than bed level elevation in the outer estuary. The Oer-IJ scenario is located at lower bed level elevation compared to similar river discharges in the straightened

and idealized trumpet scenarios in both the inner and outer estuary. Moreover bed level elevation increase as function of river discharge is smaller in the Oer-IJ. The bed level elevation increase is roughly 1 meter every 200 m^3/s river discharge for straightened and idealized trumpet scenarios. Similar to the intertidal area graph, this graph also shows a slight dip at 180 m^3/s with less variation between different scenarios.

The differences in all parameters except braiding index, but mainly in tidal range and mean absolute discharge between either the Oer-IJ shaped scenarios and both the straightened and idealized trumpet scenarios for high river discharge scenarios are large. These differences lead to the hypothesis that the sharp bends in the Oer-IJ estuary cause the estuary to behave different compared to the more straight estuary shapes, in particular when river discharge is sufficient. This hypothesis, the effects on it on this study and the assumptions on which this hypothesis is build will be discussed further in the discussion.

Effect of variables on numerical parameters

The effect of alfabn in all scenarios is minor, in particular compared to river discharge or estuary shape. The effect of alfabn is most pronounced for cross-sectional area of the mouth. Most important aspect in the results of alfabn is the lack of a trend. For all parameters the scenarios with an alfabn of 1 and an alfabn of 100 resemble each other while the reference alfabn of 10 is the off positioned scenario. This effect is unexpected and will be discussed further.

The effect of tidal components on the numerical parameters is small too, in particular compared to river discharge of estuary shape variation, despite it is slightly larger compared to alfabn. Within these figures the effect of different tidal components is different. The lack of the O1 component causes a reduction of mean absolute discharge and tidal range but only without the removal of the M4 component. A lack of M4 component causes and increased bed level elevation and percentage of intertidal area, in particular in the inner estuary. Overall the lack of both O1 and M4 results in lower values although exceptions exist (tidal range and mean absolute discharge).

Discussion

This discussion will first focus on the model results, thereafter this will focus on the effect of the modelling results on the Oer-IJ estuary itself.

The effect of river discharge

From the modelling results it was concluded that the river discharge was correlated with bed level elevation, whereas a higher river discharge correlates with a higher bed level elevation. This relation is that strong that it can trigger other relations as well.

The initial bed profiles used in the final model runs are dependent on river discharge (Table 1, Figure 19) as different river discharge scenarios have a different initial bed level elevation. However initial bed level elevation was generated based on the mean bed level elevation after 400 years on a 2 times coarser grid (each coarse cell consist of four fine cells) for each discharge and shape scenario. As a result initial bed level elevation is uniform over width but varies over the length of the estuary and results in general lower bed level elevation at narrow parts of the estuary and higher bed level elevation in wider parts of the estuary. As all model runs show that morphology is formed primary in the first 100 years the effect of initial bed elevation is more important on the formation of future bed level elevation and morphology than was expected on forehand. The effect of bed level elevation has been evaluated in the post-processing where several bathymetries were switched, both between different shape as well different river discharge. However results of these post-processing reference runs were different from the results of the full model runs. As such no value can be given to these results and it is advised to investigate these with full model runs, a research which is beyond the scope of this thesis.

The effect of river discharge is dominant in several parameters. An increased river discharge causes a decreased cross-sectional area. Cross-sectional area of the mouth has a linear relation with tidal prism (van de Kreeke 2004). Thus it is expected that a relation exist between cross-sectional area at the mouth and tidal prism. However our results stated no relation between mean absolute discharge and river discharge for the idealized trumpet and straightened scenarios, which is contrasting. A direct plot between cross-sectional area and mean absolute discharge (Figure 25) verified the lack of a linear relation.

River discharge is dominant is also the dominant variable in braiding index in the outer estuary. This effect can be related with results on river studies that indicate higher braiding index after high discharge events (Marra et al. 2014), however the environmental settings are different and in our scenario discharge is not varied over time.

High river discharge is related to high flow velocities (Kleinhans 2006), a relation which is found within this research too. Combined with a higher tidal prism, this indicates that more water is stored at high tide with high river discharge compared to low river discharges. As a result either an increased water level or an increased area is needed. Our results showed that high water levels increased with higher river discharges, a result that is countered with an increased bed level elevation with higher river discharge. As such the intertidal area cannot purely be explained by an increased river discharge.

All model runs showed an increased high (and low) water level at the upstream part of the model. This water level was further increased with more river discharge. At first an increased river discharge causes more water to flow through the inflow boundary. As the width of the inflow boundary is fixed, either the water depth has to increase or the flow velocity has to increase. Flow velocities are reduced due to tidal movement at sea and therefore the water level has to increase. This effect is primarily active at high water, however at low water this effect is still active when flow velocities cannot be increased too much.

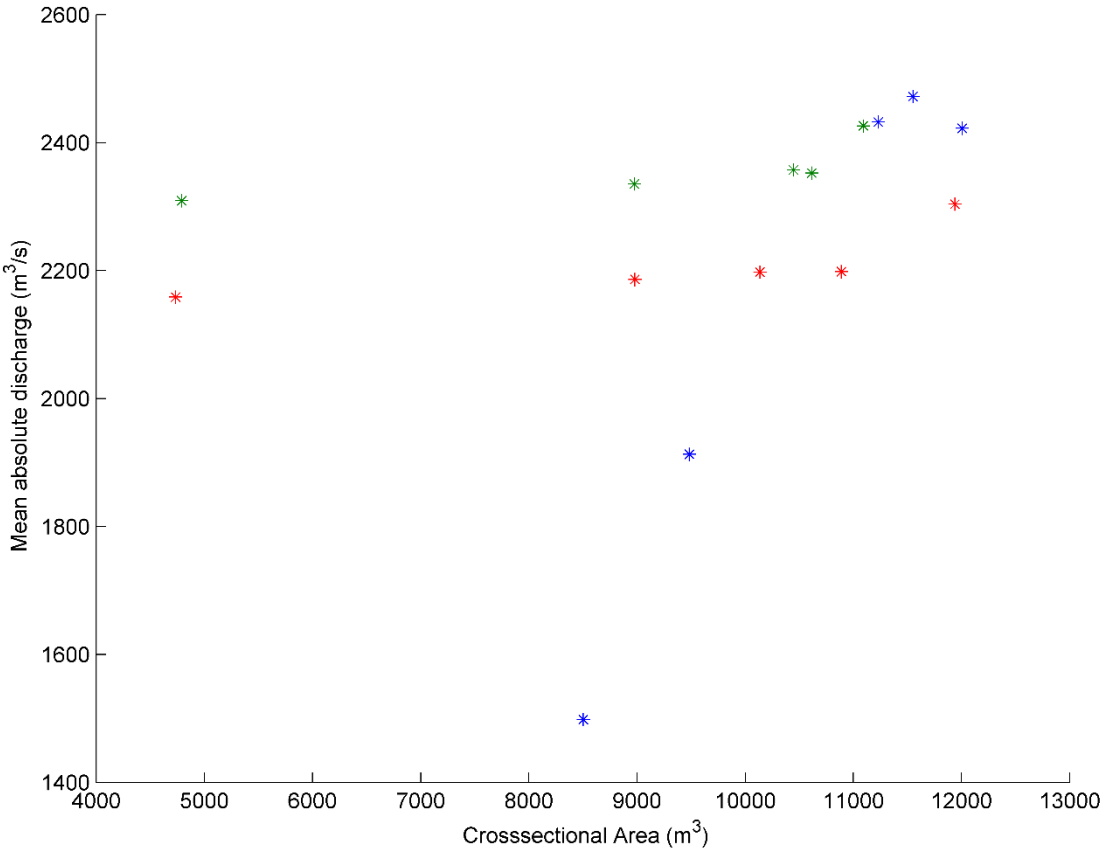

Figure 25: Mean absolute discharge as function of cross-sectional area. Colors indicate Oer-IJ (blue), straightened (red) and idealized trumpet (green) shapes.

The effect of estuary shape

In this study the effect of estuary shape was chosen to be represented by an irregular bended Oer-IJ shape, a straightened shape and an idealized trumpet shape. The research showed that differences between the straightened and the idealized grid were small and in particular trends and averaged parameters were very similar. The main difference between these two scenarios exist in the mouth of the estuary, this mouth was slightly smaller in the straightened model runs due to previous overlooked effects due orthogonalization. An decreased estuary mouth width results in a slightly smaller tidal prism. Next to that the differences between the two scenarios exist mainly in the irregularity of the straightened scenario, this effect is mainly seen in variations in bed level elevation but also the variations or stepwise behavior of the parameters of braiding index or intertidal area. This effect however, cannot be found in the estuary wide settings, as most parameters are averaged, nor is this effect seen in water levels and water level behavior. As such it can be assumed that the an idealized trumpet scenario is just as good to predict estuary-wide behaviors of an estuary that is irregular.

In the above discussion the Oer-IJ was not mentioned. Whereas the idealized trumpet scenario is a good representation for an irregular straightened estuary, it does not represent the Oer-IJ estuary in the majority of parameters and trends. Both scenarios differ a lot, in particular regarding water level and bed level elevation and in particular at higher river discharges. Two parameters which are likely to be

imposed by the initial bed level as mentioned in the previous section on the effect of river discharge. Like these scenarios, initial bed level is different for each water level. However unlike the straightened scenarios both the Oer-IJ and the idealized scenarios was given a similar bathymetry, a bathymetry purely based on the coarser grid runs of the Oer-IJ itself. Although both scenarios had a similar initial starting bathymetry, the bathymetry evaluated different in both scenarios. The idealized trumpet scenario evaluated to a scenario which final bathymetry is very similar to the straightened scenario. The difference between the Oer-IJ and the idealized trumpet scenario is as such only determined by two variations. At first the bends of the center line in the Oer-IJ compared to the straight idealized trumpet scenario and next to that the lack of irregularity in width in the idealized scenario compared to the irregular with in the Oer-IJ scenario. As the difference between an irregular (straightened) and regular (idealized trumpet) width was very minor it is assumed that the main differences are caused primarily by the bended shape of the estuary.

In the results it was shown that the differences exist in many parameters; the Oer-IJ scenarios result in a lower tidal range, lower tidal prism, lower percentage of intertidal area, lower bed level elevation, higher low water level and a higher cross-sectional area. Of these parameters it is assumed that either bed level elevation or water level is the main effect of these bends, the other parameters are related to either water level or bed level. The increased low water level and thereby reduced tidal range induces that tidal dynamics are small in the upstream area of the model. Moreover the tides have to be dampened significantly. On another note, differences in the results are in particular pronounced at higher river discharges. Higher discharges which results in a higher high water and a slightly increased low water level. Next to that higher river discharges increase the residual flow velocity over the entire estuary but in particular in channels. Differences between flow velocity for Oer-IJ and idealized scenario exist at high river discharge, high residual flow velocity shifts more from one side to the other in the Oer-IJ scenario and splits more in the idealized trumpet scenario. The shift in the Oer-IJ scenario can be related to the topographic bends where the residual flow focuses primarily in the inner bends in seaward direction.

In short higher discharge can explain why low water levels in the upstream part of the estuary are high, as water is transported downstream. However this can only be reached when the tides are reduced significantly, which cannot directly be explained by higher discharge alone.

Apart from the river, water movement is initiated from the seaward boundaries too. This tidal waves propagates into the estuary and in propagate up to the river boundary in the straightened and idealized scenarios. In the Oer-IJ scenario this propagation is not straightforward, the tidal wave has to follow the bends of the Oer-IJ. When the tidal wave propagates through a bend it can either reflect on the outer bend or it can propagate further in a slightly deformed form. When the tidal wave reflects at the outer bend the wave behaves itself like in a short estuary. In such estuary a standing wave is created, thereby creating nodes and antinodes (no tidal range and large tidal range). This effect is however not explained by the results as tidal range remains constant before the decrease.

The actual dampening takes place in between the second and third bend from the estuary mouth. At this location low water level is increased rapidly with a similar high water level. At this location the Oer-IJ scenario changes from a single channel of seaward residual flow towards multiple channels of seaward residual flow, moreover seaward of this location even the high discharge scenario has also landward directed residual flow. As such it is assumed that the tidal wave is dampened by the seaward flow of the river, a mechanism that can be enhanced due the angle between both the tidal wave as well the river

flow. It is advised that this assumption has to be tested to indicate the precise physical mechanisms and interaction at this location.

The effect of other variables

This report showed that other tested variables had a minor influence on model results in particular when compared to the effects of river and shape. Alfabn was chosen as a parameters as it influenced the model runs most in the preceding model runs on coarser grids. The results of the final model runs contradict these, although it can be addressed to differences in grid size between initial and final grid. However this assumption can only explain why there is a minor difference between different alfabn parameters, it is not convincing to explain the resemblance between both high and low alfabn values. As such it is expected that both model runs were run with similar alfabn values for the first 9 months (the alfabn model runs were amongst the runs that had to be restart due technical issues) but a different alfabn for the last 3 months. It is strengthened by the minor effects of variables in the last part of the model which was shown in the results. As such further research is needed to understand the effect of this parameter, it is also advised to combine different effects of alfabn with the high discharge scenario in the Oer-IJ where effects are possibly enhanced.

The tidal components chosen represent present day water level motion at the location of the Oer-IJ. The used tidal components (M2, M4 and O1) represent the diurnal tide (M2), the deformation of the diurnal tide (M4) and the daily inequality (O1). Moreover it is advised to keep the different components as a multitude of each other, although this decreases the reality it will increase the post-processing as it causes a more repetitive signal. The used components represent not the entire tidal signal, therefore it is debatable to add other components to the model. As the effect of the removal of one or multiple components was small it is expected more components will not change the results significantly. One exception can be the lunar component that creates the spring-neap cycle, as this result primarily in an enhanced tidal range over an period longer than a day.

Correlating modelling results to geologic reconstruction of the Oer-IJ

So far this modelling study looked primarily at the effect of the scenarios itself. Nevertheless the modelling study was based on the geologic reconstruction of the Oer-IJ. As such it is important to relate the model results with the geologic reconstruction.

At first sight the modelling results are not very similar to the geologic reconstruction. The modelling results show braided patterns that cannot be found in the geologic reconstruction. However when taken into account that the modelled part of the estuary (intertidal and subtidal areas) is the part of the reconstruction that is mostly based upon interpretation of data outside this part of the estuary. As such bar patterns are different and the focus of comparing patterns inside the estuary should be focus on large scale patterns. In the modelling studies most scenarios showed a large channel at the southern part of the estuary, a channel that follows inner bend of the first bend in the estuary. The reconstruction found the main channel at the southern part at the estuary mouth too, although it was positioned more in the center of the estuary thereafter. This was based primarily on cores at the location of the estuary mouth (Vos et al. 2010; Vos 2014) and on the location of last active channel, in particular at the 750 BC timeslice (Figure 3). Further landward the modelling studies show a single channel which is in comparison with the reconstruction. In contrast to the model the reconstruction indicate tidal creeks, part of these creeks are documented precisely by remnants in the landscape (Figure 1). The effect of these creeks is neglected in the modelling study, whereas these creeks account for storage area at high tide too, they are also more

susceptible to erosion compared to the model. In the model erosion cannot take place outside the confined estuary shape.

However one of the main hypothesis related the discharge regime of the Vecht river to the reopening and closure of the Oer-IJ estuary. This hypothesis has been tested in the modelling study where a declining Vecht discharge was modelled by a decreasing hydrograph from 180 m^3/s to 0 m^3/s in 400 years. The results of this scenario showed no clear difference between constant river discharge scenarios as the reduced river discharge was not effective to alter higher river discharge in the beginning of the model. It can be concluded that the estuary was not able to close off with this river discharge alone, nor with a constant river discharge. Whereas 180m^3/s is not the maximum river discharge of the Vecht river, future runs are optional although a closure is not expected as none of the model scenarios closed off.

The other hypothesis is related to the opening of the Vlie inlet, this inlet opened roughly at the closure of the Oer-IJ estuary. This has been modelled by a sudden decrease of river discharge. Like the fading decrease of river discharge scenario the sudden decrease scenario showed no closure nor large differences with the reference scenario.

Neither of the modelling scenarios showed the closure of the estuary, therefore it is most likely that another factor dominated or at least stimulated the closure of the estuary too. An important parameter would be alongshore sediment transport. In particular in studies regarding tidal inlets this was shown to be an important factor regarding sediment transport over the mouth of the tidal inlet (van de Kreeke 2004). Next to that possibilities exist for enlarging the model to include the freshwater lake areas as well the opening to the Waddensea and North Sea. Such model however needs to be simplified but has the possibility to determine the timing of the opening of the Vlie-inlet in relation to the closure of the Oer-IJ estuary.

The last characteristic of the geologic reconstruction was succession of two periods of activity (2500 – 1000 BC and 650 – 200 BC) separate by a period of minor activity. This part of the reconstruction was mainly based on a decreased high water level and as such a decreased tidal range (Vos 2014) and a reduction in cross-sectional area of the estuary mouth (Vos et al. 2010). In contrast to these assumptions our results show a relation between river discharge and both cross-sectional area of the mouth and tidal range. With an increased river discharge both the cross-sectional area and the tidal range decrease significantly (Figure 24). This assumes that the estuary itself did not close off between 1000 and 650 BC and instead had an increased river discharge. This assumption is strengthened by discharge data of the Vecht river system, which was adopted at 1000-950 BC (Bos et al. 2009).

On the contrary the model results showed increased low water level at the Oer-IJ scenarios in the inner part of the estuary. Whereas exact dynamics behind this effect are yet unclear, correlations with archeologic and geologic data can be made. At roughly 15-20 kilometer from the estuary mouth, near present day Beverwijk, a roman encampment was found, including a small harbor. Amongst archeologists the question arises why this location was chosen for this encampment as a location closer to the open sea was opted to be more favorable (Vos 2014). This location however correlates relative good with the model results, tidal range was reduced significantly in high discharge scenarios from 10 – 15 kilometer from the mouth. As such the hypothesis arise whether the roman encampment was built at that location due to the reduction in tidal range. However that is beyond the scope of this thesis.

Conclusion

The combination of geology and numerical modelling in an estuarine environment, with focus on the Oer-IJ estuary, showed clear relations in combination with refreshing though unexpected outcomes despite several expectations were not met.

The effect of river discharge was primary shown in three aspects. At first high and low water levels increased slightly with increased river discharge, meanwhile tidal range remained unchanged. Secondly the estuary shows more bars and becomes more braiding in the outer estuary with an increased river discharge. And thirdly an increased river discharge resulted in an increased bed level elevation.

The shape of the estuary resulted in clear contrast between different scenarios. Idealized scenarios are a valid representation for irregular shaped but straight estuaries. Idealized scenarios are not a valid representation for the bended Oer-IJ. The effect of the bended estuary is refreshing. With no or low river discharge the estuary behaves rather similar. With higher river discharges the estuary the tides are dampened rapidly in the center of the estuary.

The effect of alfabn parameter and variation in tidal components was minimal compared to river discharge and estuary shape.

References

Blanckaert, K. et al., 2013. Flow separation at the inner (convex) and outer (concave) banks of constant-width and widening open-channel bends. *Earth Surface Processes and Landforms*, 38(7), pp.696–716.

Bos, I.J., 2010. Architecture and facies distribution of organic-clastic lake fills in the fluvio-deltaic Rhine-Meuse system, The Netherlands. *Journal of Sedimentary Research*, 80(4), pp.339–356.

Bos, I.J. et al., 2009. Influence of organics and clastic lake fills on distributary channel processes in the distal Rhine-Meuse delta (The Netherlands). *Palaeogeography, Palaeoclimatology, Palaeoecology*, 284, pp.355–374.

Brown, J.M. & Davies, a. G., 2010. Flood/ebb tidal asymmetry in a shallow sandy estuary and the impact on net sand transport. *Geomorphology*, 114(3), pp.431–439.

Coeveld, E.M., 2002. Feedback mechanisms in channel-shoal formation.

Dam, G. et al., 2007. Long term process-based morphological model of the Western Scheldt Estuary. In *Proceedings of the 5th IAHR Symposium on River, Coastal and Estuarine Morphodynamics*.

Deltares, 2011. Simulation of multi-dimensional hydrodynamic flows and transport phenomena, including sediments. In *Delft3D-FLOW, user manual*.

Engelund, F. & Hansen, E., 1967. A monograph on sediment transport in alluvial streams. *Teknisk Forlag*.

Hibma, a., de Vriend, H.J. & Stive, M.J.F., 2003. Numerical modelling of shoal pattern formation in well-mixed elongated estuaries. *Estuarine, Coastal and Shelf Science*, 57(5-6), pp.981–991.

Kalkwijk, J.P.T. & Booij, R., 1986. Adaptation of secondary flow in nearly-horizontal flow. *Journal of Hydraulic Research*, 24(1), pp.19–37.

Kleinhans, M.G., 2006. Correction to “Flow discharge and sediment transport models for estimating a minimum timescale of hydrological activity and channel and delta formation on Mars.” *Journal of Geophysical Research*, 111(E1), p.E12003.

Kleinhans, M.G., Weerts, H.J.T. & Cohen, K.M., 2010. Avulsion in action: Reconstruction and modelling sedimentation pace and upstream flood water levels following a Medieval tidal-river diversion catastrophe (Biesbosch, The Netherlands, 1421–1750AD). *Geomorphology*, 118(1-2), pp.65–79.

Koch, F.G. & Flokstra, C., 1980. Bed level computation for curved alluvial channels. *Proceedings of the XIXth congress of the international association for Hydraulic Research, New Delhi, India*, 2, pp.357–364.

Van de Kreeke, J., 2004. Equilibrium and cross-sectional stability of tidal inlets: application to the Frisian Inlet before and after basin reduction. *Coastal Engineering*, 51(5-6), pp.337–350.

Lesser, G.R. et al., 2004. Development and validation of a three-dimensional morphological model. *Coastal Engineering*, 51(8-9), pp.883–915.

Marra, W. a., Kleinhans, M.G. & Addink, E. a., 2014. Network concepts to describe channel importance and change in multichannel systems: test results for the Jamuna River, Bangladesh. *Earth Surface Processes and Landforms*, 39(6), pp.766–778.

Ranasinghe, R. et al., 2011. Morphodynamic upscaling with the MORFAC approach: Dependencies and sensitivities. *Coastal Engineering*, 58(8), pp.806–811.

Van Rijn, L.C., 1993. *Principles of sediment Transport in River, Estuaries and Coastal seas.*,

Van Rijn, L.C., 2007. Unified View of Sediment Transport by Currents and Waves. I: Initiation of Motion, Bed Roughness, and Bed-Load Transport. *Journal of Hydraulic Engineering*, 133(6), pp.649–667.

Robins, P.E. & Davies, A.G., 2010. Morphological controls in sandy estuaries: the influence of tidal flats and bathymetry on sediment transport. *Ocean Dynamics*, 60(3), pp.503–517.

Roelvink, D. & Walstra, D.-J., 2004. Keeping it simple by using complex models. *Advances in Hydro-science and -engineering*, VI, pp.1–11.

Van der Spek, A.J.F., 1995. Reconstruction of tidal inlet and channel dimensions in the Frisian Middelzee, a former tidal basin in the Dutch Wadden Sea. *Spec. Publs int. Ass. Sediment.*, 24, pp.239–258.

Stive, M.J.F. & Wang, Z.B., 2003. Chapter 13 Morphodynamic modelling of tidal basins and coastal inlets. In *Elsevier Oceanography Series*. pp. 367–392.

Teske, R., 2013. *Tidal inlet channel stability in long term process based modelling*.

Vos, P.C. et al., 2011. *Atlas van Nederland in het Holoceen*,

Vos, P.C., 2000. *Geo-archeologisch profiel Broekpolder 1999*,

Vos, P.C., 2014. Personal conversation.

Vos, P.C., 2012. The Oer-IJ estuary – geology and morphodynamics shaping the landscape.

Vos, P.C., van Eerden, R.A. & de Koning, J., 2010. *Paleolandschap en archeologie van het PWN duingebied bij Castricum*,

Van der Wegen, M., 2013. Personal conversation.

Van der Wegen, M., Dastgheib, A. & Roelvink, J. a., 2010. Morphodynamic modeling of tidal channel evolution in comparison to empirical PA relationship. *Coastal Engineering*, 57(9), pp.827–837.